Appendix for manuscript:

Global projections of potential lives saved from COVID-19 through universal mask use

IHME COVID-19 Forecasting Team

Section 1. Estimating the effectiveness of masks in preventing transmission

Data Extraction

In total, 63 rows of data from 40 unique publications were extracted; one article (Pei) had an unclear comparison group and is thus missing the `ControlGroup` variable. Given that it did not have complete data, it was removed from analyses, but included in a sensitivity analysis, resulting in 62 rows of data from 39 unique publications. All publications were traced and translated, when published not in English.

The following variables were of particular interest for the data extraction:

- `GeneralPop`: Type of population using the mask (General Population (1) versus Healthcare Population (0))
- `SE_Asia`: Country of study (SE Asian countries (1) vs non- SE Asian countries (0))
- `OtherMask`: Type of mask (Paper / Cloth or non-descript masks (1) versus medical masks and N95 masks (0))
- `NoMaskControl`: Type of control group (No use (1) versus infrequent use (0))
- `Dx`: Disease (SARS-CoV 1 or 2 (1) versus H1N1 / Influenza/ other Respiratory pathogens (0))
- `ClinicalDx`: Type of diagnosis (Clinical (1) versus Laboratory (0))
- `Study_type`: Study type (case contro versus clustered randomized control trial (RCT) and cohort)

We extracted all relevant data to form 2x2 tables and calculated the Relative Risks and corresponding (log-transformed) Standard Errors for use in our MR-BRT analysis.

IHME's customized meta-regression tool MR-BRT. MR-BRT ("meta-regression—Bayesian, regularized, trimmed") is a trimmed constrained mixed-effects model that provides an easy interface for formulating and solving common linear and nonlinear mixed effects models. It is open source, and its core computational kernel uses the mixed effects package LimeTr (https://github.com/zhengp0/limetr) and the spline package XSpline (https://github.com/zhengp0/xspline). For the statistical models and algorithmic features underlying MR-BRT, a published technical report is available here: https://arxiv.org/abs/1909.10700 .

In order to account for between-study heterogeneity, we included a gamma term to reflect this heterogeneity in the uncertainty interval. MR-BRT also relaxes the assumption that there is one "true" point estimate across all studies and instead allows for variation in the point estimate.

MR-BRT Analysis

Following data extraction, we used MR-BRT to do a meta-regression of the data, allowing for between-study heterogeneity using the gamma term and random effects. The following models were constructed:

- Intercept-only model (shown in univariate figure)

- All univariate associations
- Multivariate models
- Sub-analyses for key variables of interest (population and mask type)

Sensitivity analyses were also performed to test out other models and methods, including:

- Model specifications using different continuity corrections (0.5 versus 0.001)
- Fixed-effects only model
- Odds ratios versus relative risks
- Included estimates and confidence intervals from 1 study without full data – intercept only
- Looking at reported confidence interval versus calculated confidence interval for all studies, and
- Looking at results omitting any clustered RCTs

All presented analyses use the continuity correction of 0.001, present RRs rather than ORs, and include random-effects with the Gamma term. Sensitivity analyses revealed no major differences in results using a continuity correction of 0.001 versus 0.5, nor using RRs versus ORs.

SI Figure 1: Relative Risk of respiratory virus infection by publication first author and year of publication

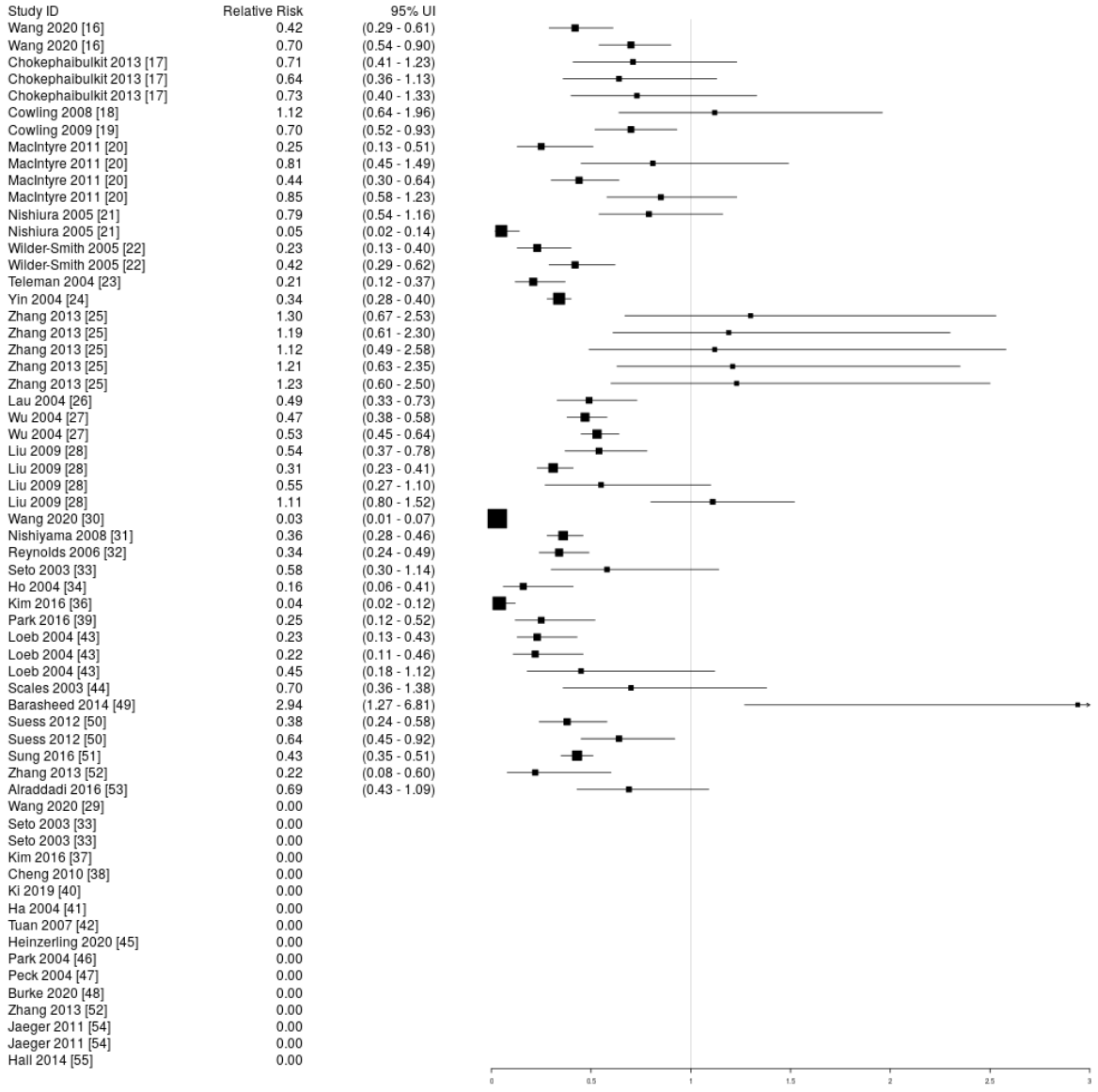

This figure demonstrates the relative risk of respiratory virus infection, recalculated for use in this meta-regression based on numbers reported in the publication. We present a RR of zero where there were zero counts in the numerator; confidence intervals were not presented for these studies in the figure. These studies were included in the analysis with a continuity correction, however.

SI Table 1: Meta-Regression Publication Characteristics

Characteristic		N (%) of Observations	Studies
Study Location*	**South-East Asia**	27 (67.5%)	16-42
	Outside South-East Asia	13 (32.5%)	43-55
Disease Studied	**SARS-CoV 1 or 2**	34 (54%)	16, 21-24, 26-35, 41-48
	Not SARS-CoV 1 or 2	29 (56%)	17-20, 25, 36-40, 49-55
Mask Type Studied	**Cloth Masks**	2 (3%)	25,35
	Non-Descript Masks	17 (27%)	16, 24-28, 31,33, 41,42,52,54
	Medical, Surgical, or N95 Masks	44 (70%)	17-23,25,28-30, 32-34, 36-40, 43-51, 53,55
Diagnosis	**Laboratory**	53 (84%)	16-22, 25, 28-32,34-38, 40-43, 45-55
	Clinical	10 (16%)	23,24,26,27,33,39,44
Population and Setting	**General**	13 (21%)	16,18,19,26,27,42,49,50,52
	Healthcare	50 (79%)	17,20-25, 28-41,43-48, 53-55
Type of Control Group	**Infrequent Mask Use**	14 (22%)	21,25,32,36,41,43,45,47,53,54
	No Mask Use	47 (75%)	16-20,22-31,33,34,37-40,42,44,46,48-50,52,54,55
	Pre- and Post-Intervention Mask Wear	1 (2%)	51
	Missing	1 (2%)	35

*This row presents the results at the study-level (N=40) rather than the observation level (N=63) as the study location did not vary within an individual study

SI Table 2: Individual publication characteristics

Author	Mask Wearers, Infection +	Mask Wearers	Mask Non-wearers, Infection +	Mask Non-wearers	Study Country	Disease	Diagnosis	Mask Type	Study Design	Healthcare Setting	Intervention Group Type	Control Group Type	Citation
Wang	8	46	17	41	China	SARS-CoV-2	Laboratory	Non-medical mask	Cohort	No	Consistent Use	No mask use	16
Wang	24	83	17	41	China	SARS-CoV-2	Laboratory	Non-medical mask	Cohort	No	Any Use	No mask use	16
Chokephaibulkit	30	239	3	17	Thailand	H1N1	Laboratory	Medical mask	Case Control	Yes	Non-medical mask	No mask use	17
Chokephaibulkit	16	142	3	17	Thailand	H1N1	Laboratory	Medical mask (N95)	Case Control	Yes	Medical mask (N95)	No mask use	17
Chokephaibulkit	10	78	3	17	Thailand	H1N1	Laboratory	Medical mask	Case Control	Yes	Medical mask	No mask use	17
Cowling	4	61	12	205	China (Hong Kong)	Influenza	Laboratory	Medical mask	cRCT	No	Facemask	No mask use	18
Cowling	18	258	28	279	China (Hong Kong)	Influenza	Laboratory	Medical mask	cRCT	No	Facemask + Hygiene	No mask use	19
MacIntyre	3	949	6	481	China	Influenza	Laboratory	Medical mask (N95)	cRCT	Yes	Medical mask (N95)	No mask use	20
MacIntyre	5	492	6	481	China	Influenza	Laboratory	Medical mask	cRCT	Yes	Medical mask	No mask use	20
MacIntyre	13	949	15	481	China	Respiratory Virus	Laboratory	Medical mask (N95)	cRCT	Yes	Medical mask (N95)	No mask use	20
MacIntyre	13	492	15	481	China	Respiratory Virus	Laboratory	Medical mask	cRCT	Yes	Medical mask	No mask use	20
Nishiura	8	43	17	72	Vietnam	SARS	Laboratory	Medical mask	Case Control	Yes	Consistent Use	Inconsistent use	21
Nishiura	1	26	3	4	Vietnam	SARS	Laboratory	Medical mask	Case Control	Yes	Consistent Use	Inconsistent use	21
Wilder-Smith	3	24	37	68	Singapore	SARS	Laboratory	Medical mask (N95)	Case Control	Yes	Any Use	No mask use	22
Wilder-Smith	6	27	34	65	Singapore	SARS	Laboratory	Medical mask (N95)	Case Control	Yes	Any Use	No mask use	22
Teleman	3	26	33	60	Singapore	SARS	Clinical	Medical mask (N95)	Case Control	Yes	Medical mask (N95)	No mask use	23
Yin	68	246	9	11	China	SARS	Clinical	Non-medical mask	Case Control	Yes	Any Use	No mask use	24
Zhang	33	152	2	12	China	H1N1	Laboratory	Non-medical mask	Case Control	Yes	Consistent Use	Inconsistent use	25
Zhang	44	222	2	12	China	H1N1	Laboratory	Non-medical mask	Case Control	Yes	Any Use	Inconsistent use	25
Zhang	3	16	2	12	China	H1N1	Laboratory	Medical mask (N95)	Case Control	Yes	Medical mask (N95)	No mask use	25
Zhang	37	183	2	12	China	H1N1	Laboratory	Medical mask	Case Control	Yes	Medical mask	No mask use	25

Zhang	9	44	2	12	China	H1N1	Laboratory	Non-medical mask	Case Control	Yes	Non-medical mask	No mask use	25
Lau	8	94	17	98	Hong Kong	SARS	Clinical	Non-medical mask	Case Control	No	Any Use	No mask use	26
Wu	25	146	44	120	China	SARS	Clinical	Non-medical mask	Case Control	No	Consistent Use	No mask use	27
Wu	50	255	44	120	China	SARS	Clinical	Non-medical mask	Case Control	No	Any Use	No mask use	27
Liu	8	123	43	354	China	SARS	Laboratory	Medical mask	Case Control	Yes	Any Use	No mask use	28
Liu	15	274	36	203	China	SARS	Laboratory	Medical mask	Case Control	Yes	Any Use	No mask use	28
Liu	2	33	49	444	China	SARS	Laboratory	Medical mask (N95)	Case Control	Yes	Any Use	No mask use	28
Liu	11	95	40	382	China	SARS	Laboratory	Non-medical mask	Case Control	Yes	Any Use	No mask use	28
Wang	0	278	10	215	China	SARS-CoV-2	Laboratory	Medical mask (N95)	Case Control	Yes	Any Use	No mask use	29
Wang	1	1286	119	4036	China	SARS-CoV-2	Laboratory	Medical mask	Case Control	Yes	Any Use	No mask use	30
Nishiyama	17	61	14	18	Vietnam	SARS	Laboratory	Non-medical mask	Cohort	Yes	Consistent Use	No mask use	31
Reynolds	8	42	14	25	Vietnam	SARS	Laboratory	Medical mask	Case Control	Yes	Consistent Use	Inconsistent use	32
Seto	2	13	26	98	China	SARS	Clinical	Non-medical mask	Case Control	Yes	Any Use	No mask use	33
Seto	0	11	51	123	China	SARS	Clinical	Medical mask	Case Control	Yes	Any Use	No mask use	33
Seto	0	11	92	164	China	SARS	Clinical	Medical mask (N95)	Case Control	Yes	Any Use	No mask use	33
Ho	2	62	2	10	China	SARS	Laboratory	Medical mask (N95)	Cohort	Yes	Any Use	No mask use	34
Pei	11	98	61	115	China	SARS	Laboratory	Non-medical mask	Case Control	Yes	MISSING	MISSING	35
Kim	1	444	16	308	South Korea	MERS	Laboratory	Medical mask (N95)	Case Control	Yes	Consistent Use	Inconsistent use	36
Kim	0	7	1	2	South Korea	MERS	Laboratory	Non-medical mask	Case Control	Yes	Any Use	No mask use	37
Cheng	0	568	4	268	China (Hong Kong)	H1N1	Laboratory	Medical mask	Case Control	Yes	Any Use	No mask use	38
Park	3	24	2	4	South Korea	MERS	Clinical	Medical mask	Case Control	Yes	Any Use	No mask use	39
Ki	0	218	6	230	South Korea	MERS	Laboratory	Medical mask	Case Control	Yes	Any Use	No mask use	40
Ha	0	61	0	1	Vietnam	SARS	Laboratory	Non-medical mask	Cohort	Yes	Consistent Use	Inconsistent use	41
Tuan	0	9	7	154	Vietnam	SARS	Laboratory	Non-medical mask	Cohort	No	Consistent Use	No mask use	42
Loeb	3	23	5	9	Canada	SARS	Laboratory	Medical mask	Case Control	Yes	Consistent Use	Inconsistent use	43

Loeb	2	16	5	9	Canada	SARS	Laboratory	Medical mask (N95)	Case Control	Yes	Consistent Use	Inconsistent use	43
Loeb	1	4	5	9	Canada	SARS	Laboratory	Medical mask	Case Control	Yes	Consistent Use	Inconsistent use	43
Scales	3	16	4	15	Canada	SARS	Clinical	Medical mask	Case Control	Yes	Any Use	No mask use	44
Heinzerling	0	3	3	34	USA	SARS-CoV-2	Laboratory	Medical mask	Case Control	Yes	Consistent Use	Inconsistent use	45
Park	0	57	0	45	USA	SARS	Laboratory	Medical mask	Cohort	Yes	Any Use	No mask use	46
Peck	0	13	0	28	USA	SARS	Laboratory	Medical mask (N95)	Cohort	Yes	Consistent Use	Inconsistent use	47
Burke	0	63	0	13	USA	SARS-CoV-2	Laboratory	Medical mask	Cohort	Yes	Any Use	No mask use	48
Barasheed	4	36	2	53	KSA	Respiratory Virus	Laboratory	Medical mask	cRCT	No	Medical mask	No mask use	49
Suess	6	69	19	82	Germany	Influenza	Laboratory	Medical mask	cRCT	No	Facemask	No mask use	50
Suess	10	67	19	82	Germany	Influenza	Laboratory	Medical mask	cRCT	No	Facemask + Hygiene	No mask use	50
Sung	40	911	95	920	USA	Respiratory Virus	Laboratory	Medical mask	Prospective Trial	Yes	Post-intervention mask period	Pre-intervention control period	51
Zhang	1	16	8	28	Airline Flight	H1N1	Laboratory	Non-medical mask	Case Control	No	Any Use	No mask use	52
Zhang	0	15	9	26	Airline Flight	H1N1	Laboratory	Non-medical mask	Case Control	No	Any Use	No mask use	52
Alraddadi	11	151	7	66	KSA	MERS	Laboratory	Medical mask	Cohort	Yes	Consistent Use	Inconsistent use	53
Jaeger	0	20	9	43	USA	H1N1	Laboratory	Non-medical mask	Cohort	Yes	Any Use	No mask use	54
Jaeger	0	12	9	51	USA	H1N1	Laboratory	Non-medical mask	Cohort	Yes	Consistent Use	Inconsistent use	54
Hall	0	42	0	6	KSA	MERS	Laboratory	Medical mask	Case Control	Yes	Any Use	No mask use	55

SI Figure 2: Univariate MR-BRT model results

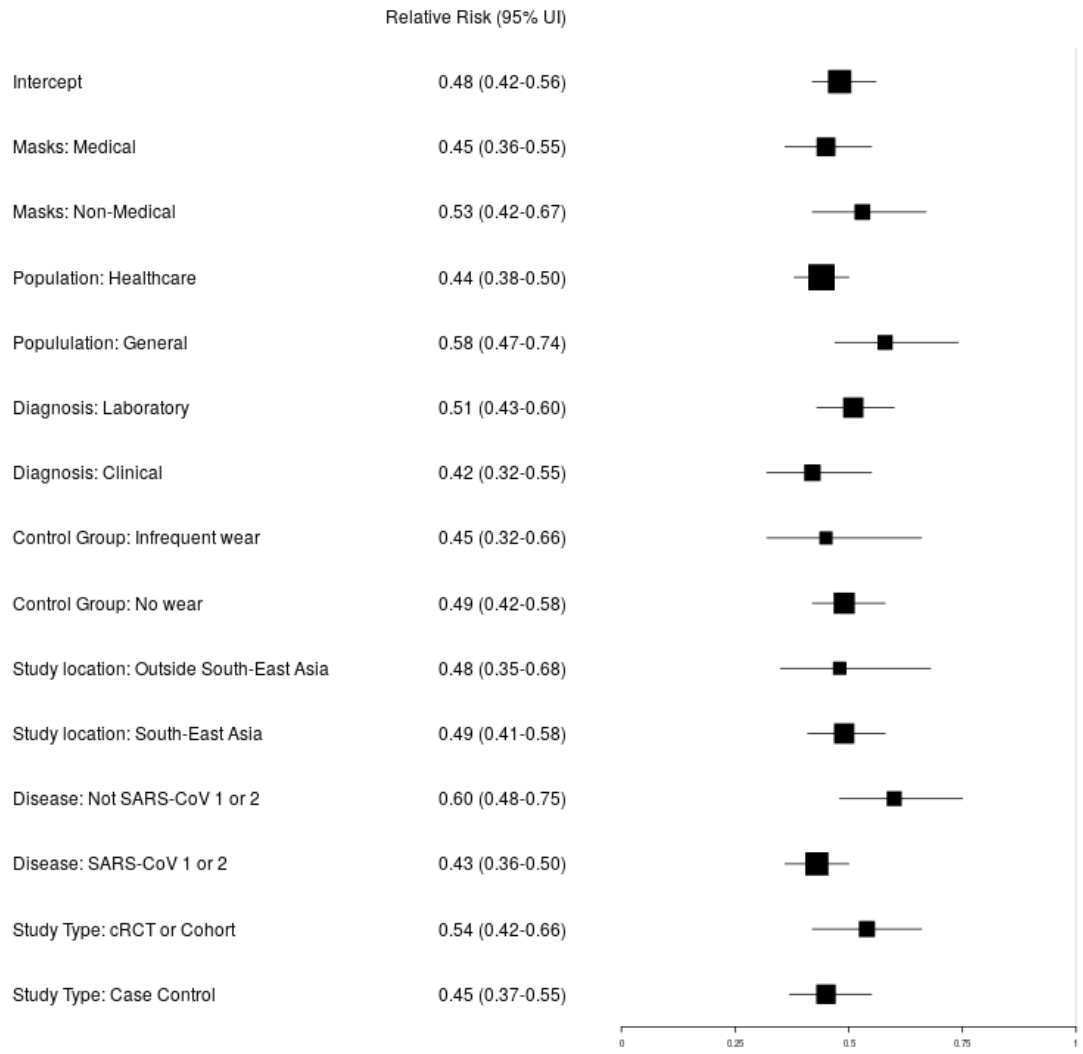

This figure depicts the relative risk (and corresponding 95% UI) for each variable of interest, separately, using meta-regression techniques; the first row presents the results of an intercept-only model. The size of the box is proportional to the precision of the estimate, based on number of observations, with more precise studies having larger boxes.

SI Figure 3: Sub analyses: (A) the estimates for non-medical mask usage among healthcare populations and general populations; (B) the estimates for general population non-medical and medical mask usage

A

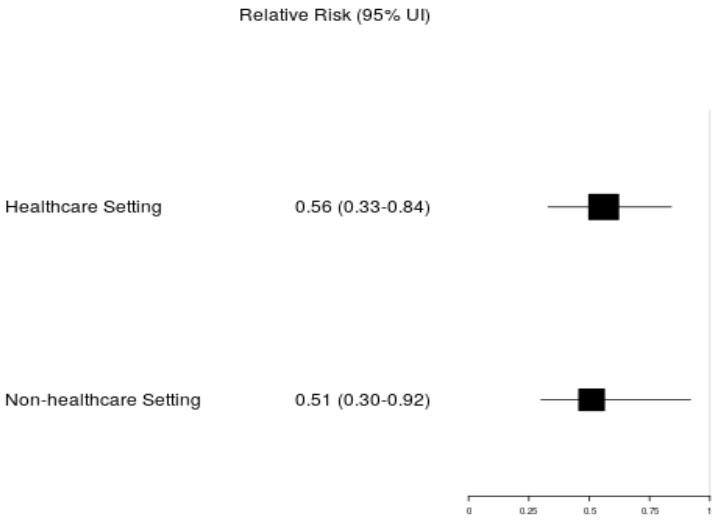

B

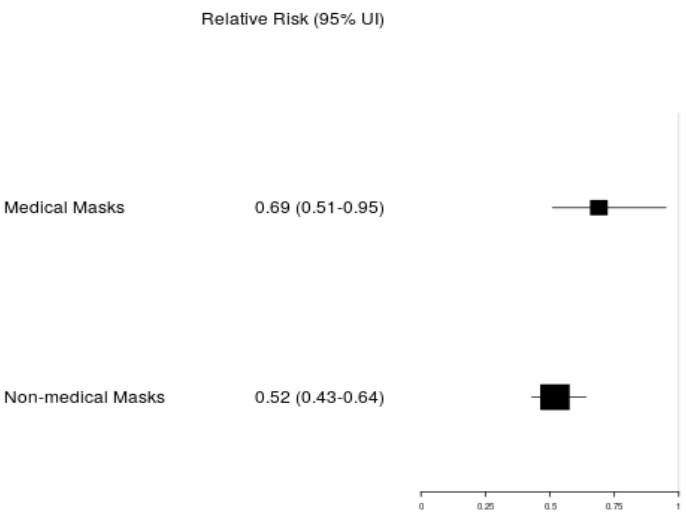

SI Figure 4: Sensitivity analysis using a continuity correction of 0.5 versus 0.01

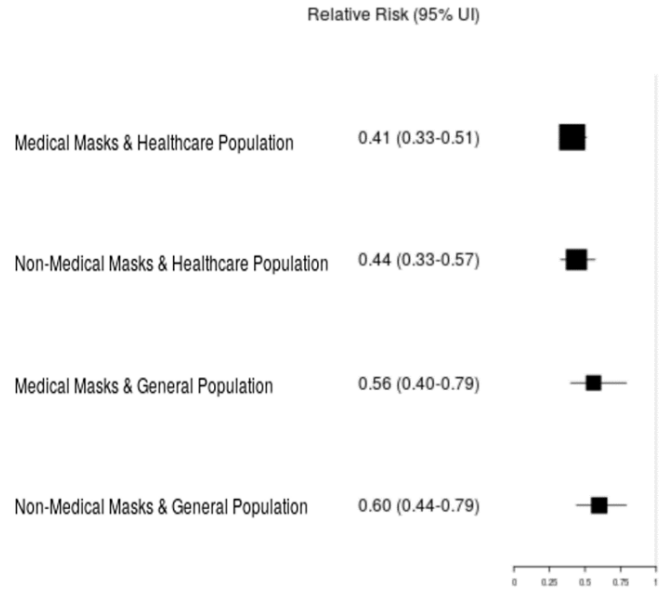

SI Figure 5: Sensitivity model using a fixed-effects model versus random-effects model

SI Figure 6: Sensitivity analysis using calculated OR versus RR

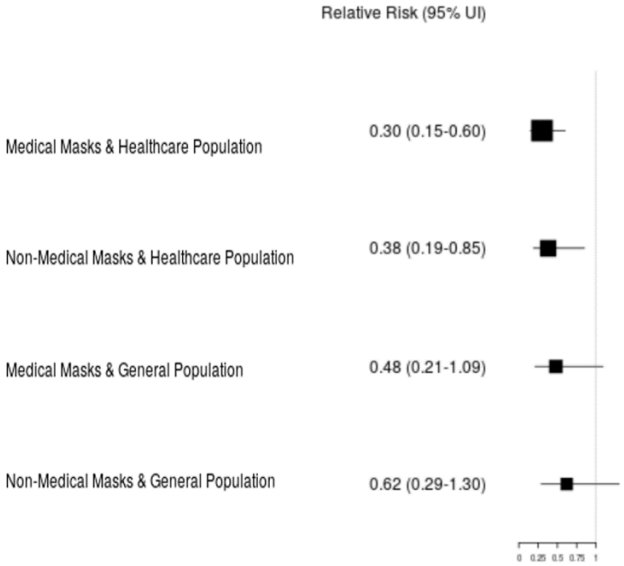

SI Figure 7: Sensitivity analysis looking at intercept-only model with all 63 observations versus those with full data

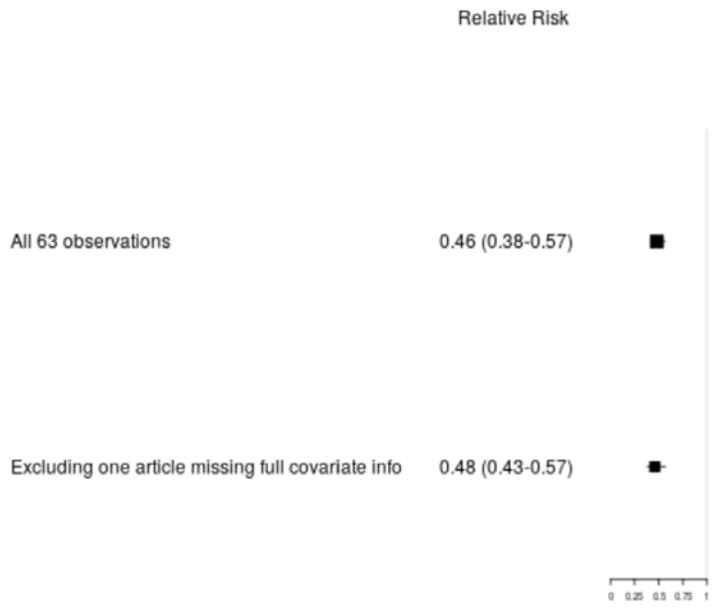

SI Figure 8: Sensitivity analysis using reported confidence interval, where available, versus calculated SE for all 63 observations

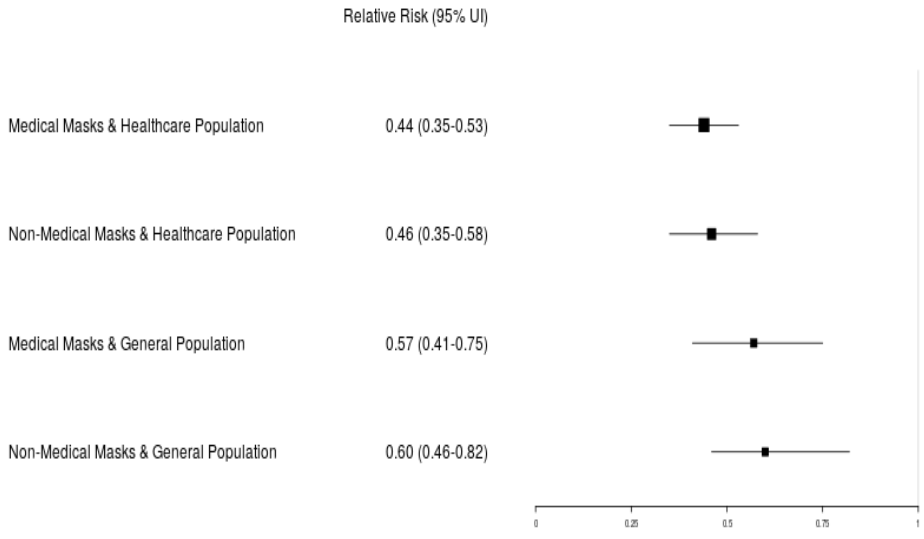

SI Figure 9: Sensitivity analysis omitting cRCTs (n=53 observations)

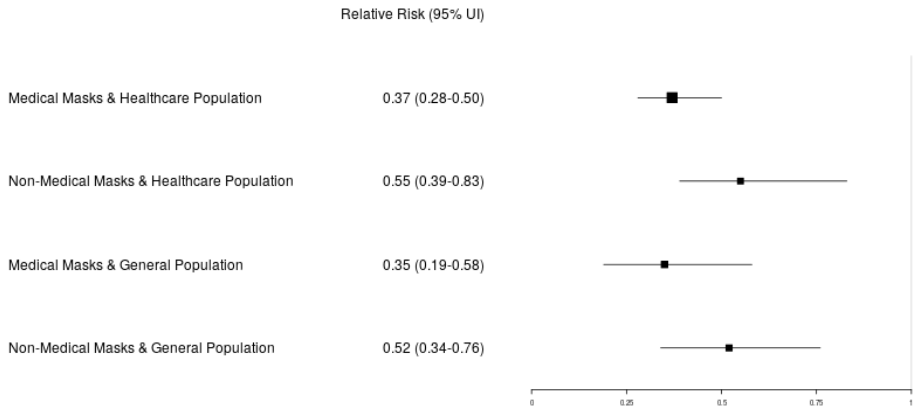

Section 2. Trends in the proportion of the population that report using a mask by select demographic characteristics of respondents and by country.

SI Figure 10: Mask use by gender globally and by GBD super region.

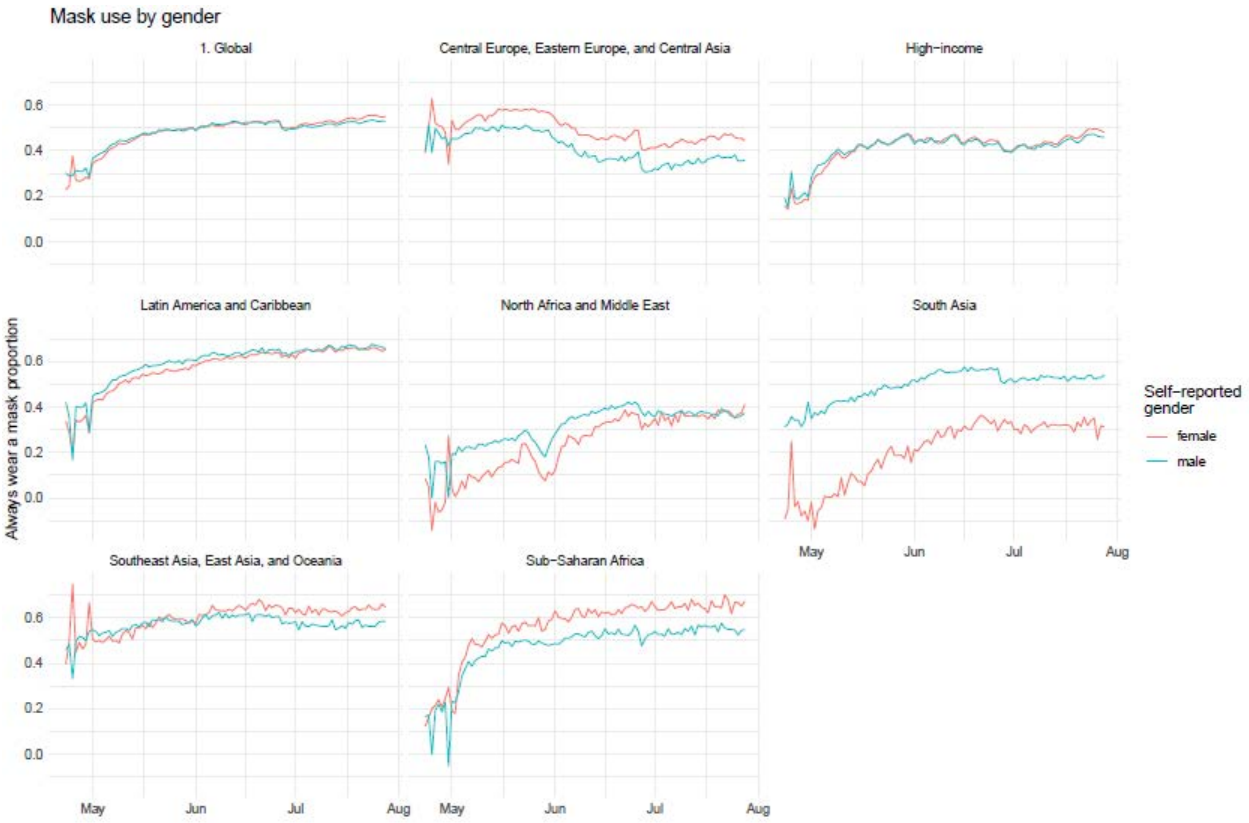

SI Figure 11: Mask use by adult age group globally and by GBD super region.

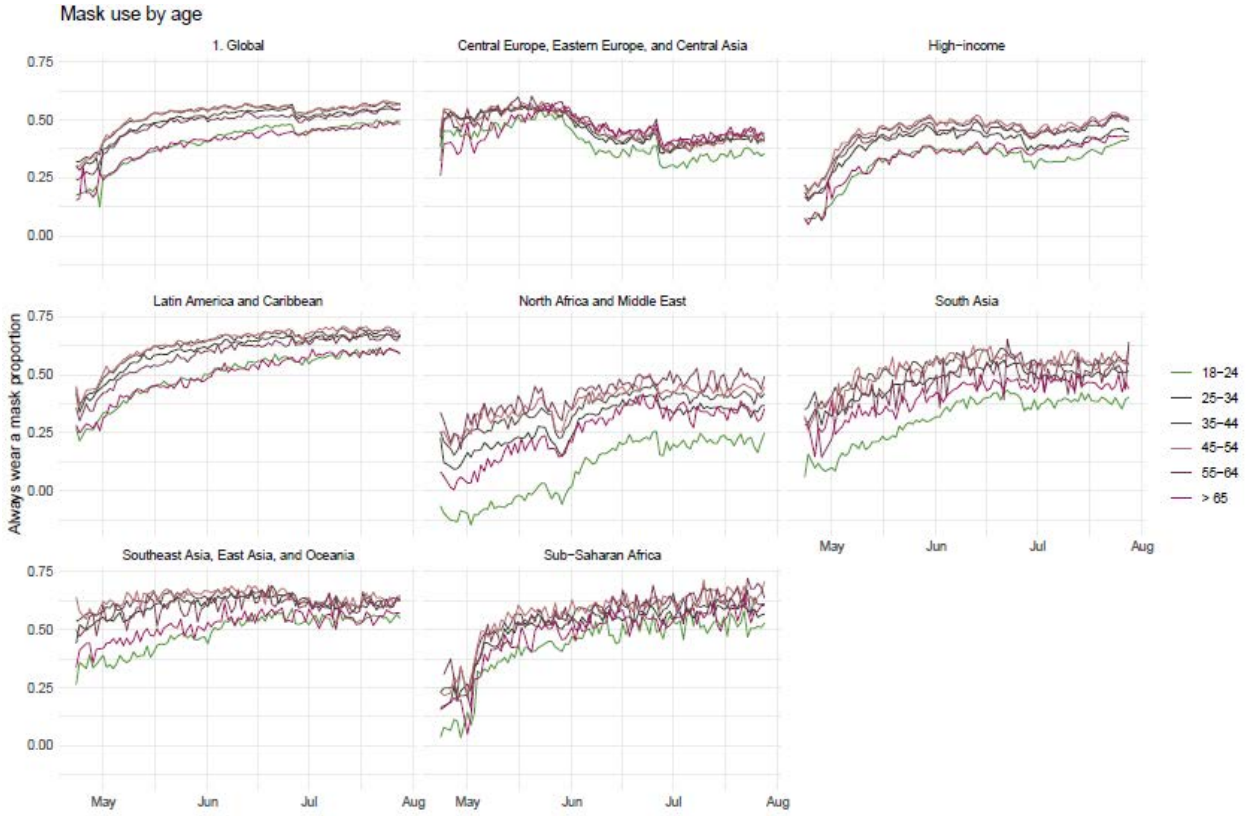

SI Figure 12: Mask use by urbanicity globally and by GBD super region.

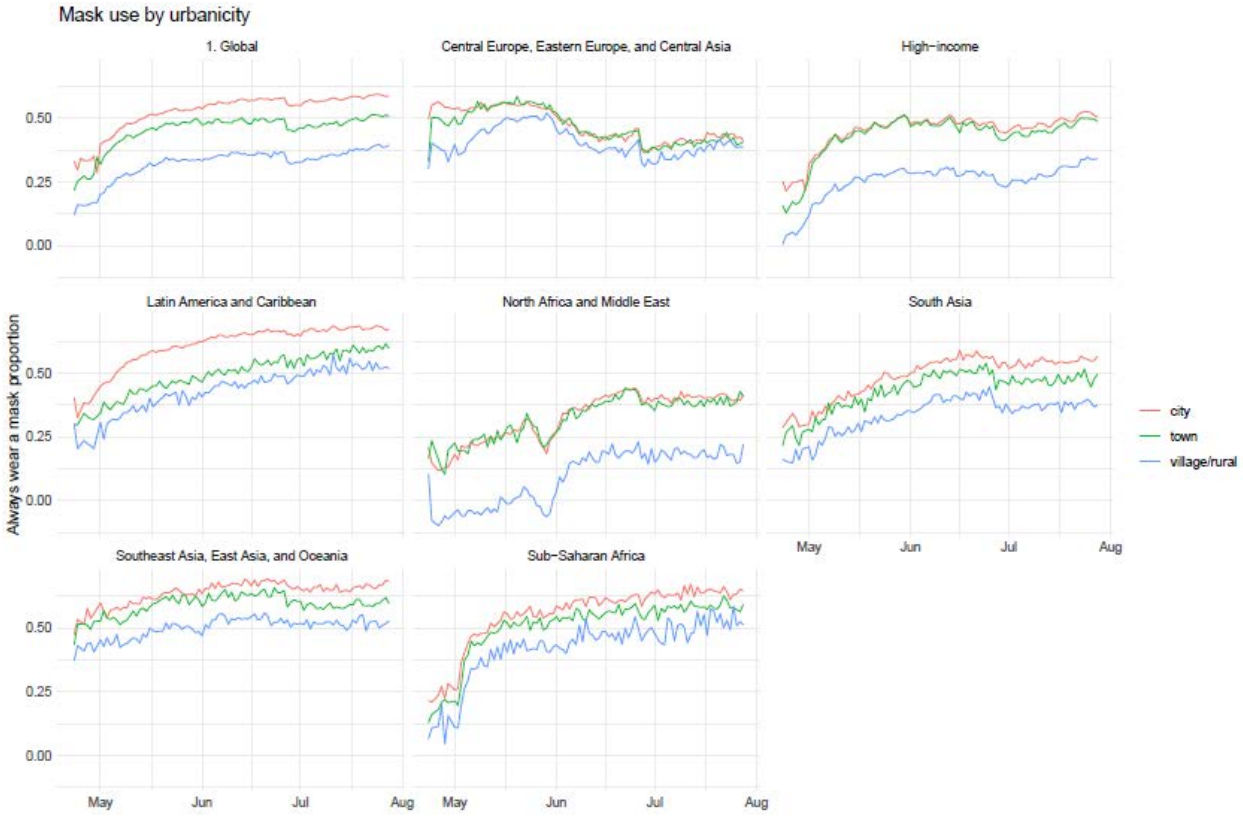

SI Figure 13: Mask use by self-reported number of contacts in the previous 24 hours globally and by GBD super region.

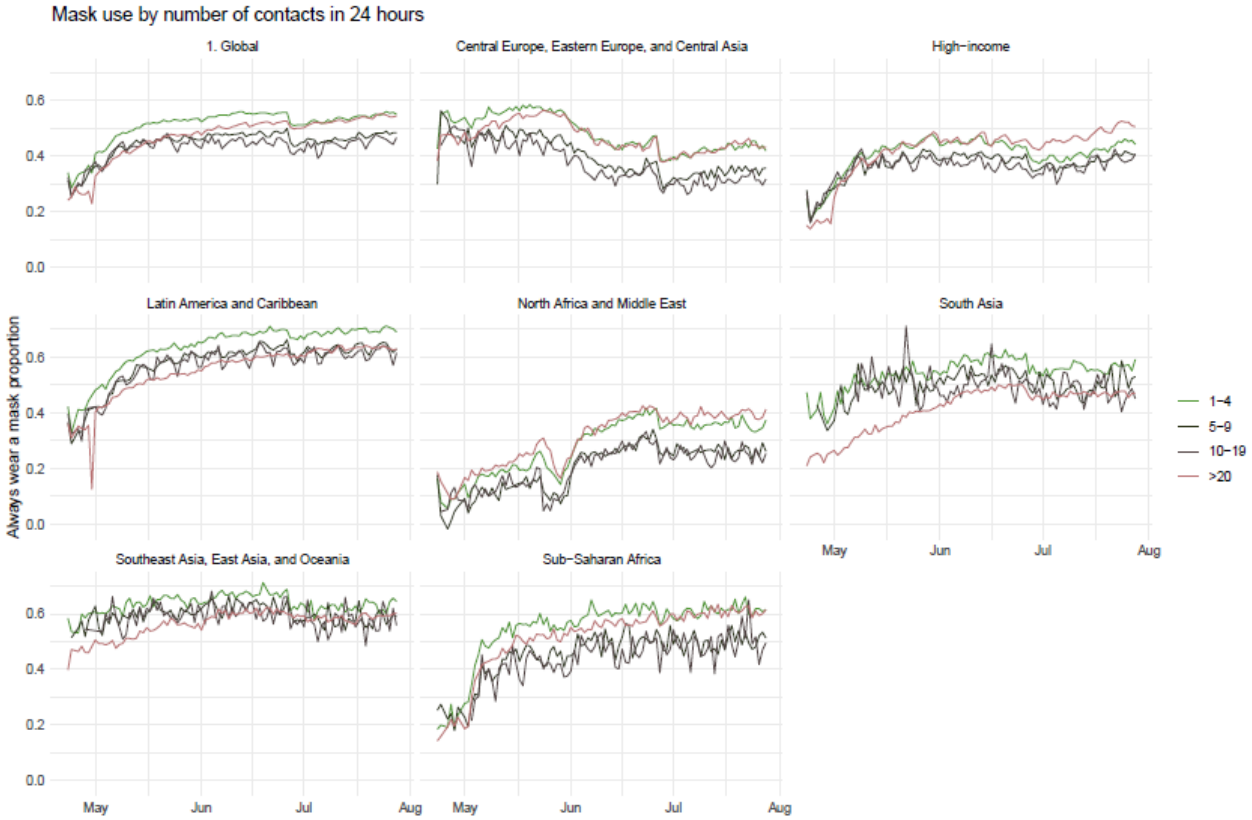

SI Figure 14: Estimates of mask use at the national level by GBD region between January 1st 2020 and January 1st 2021.

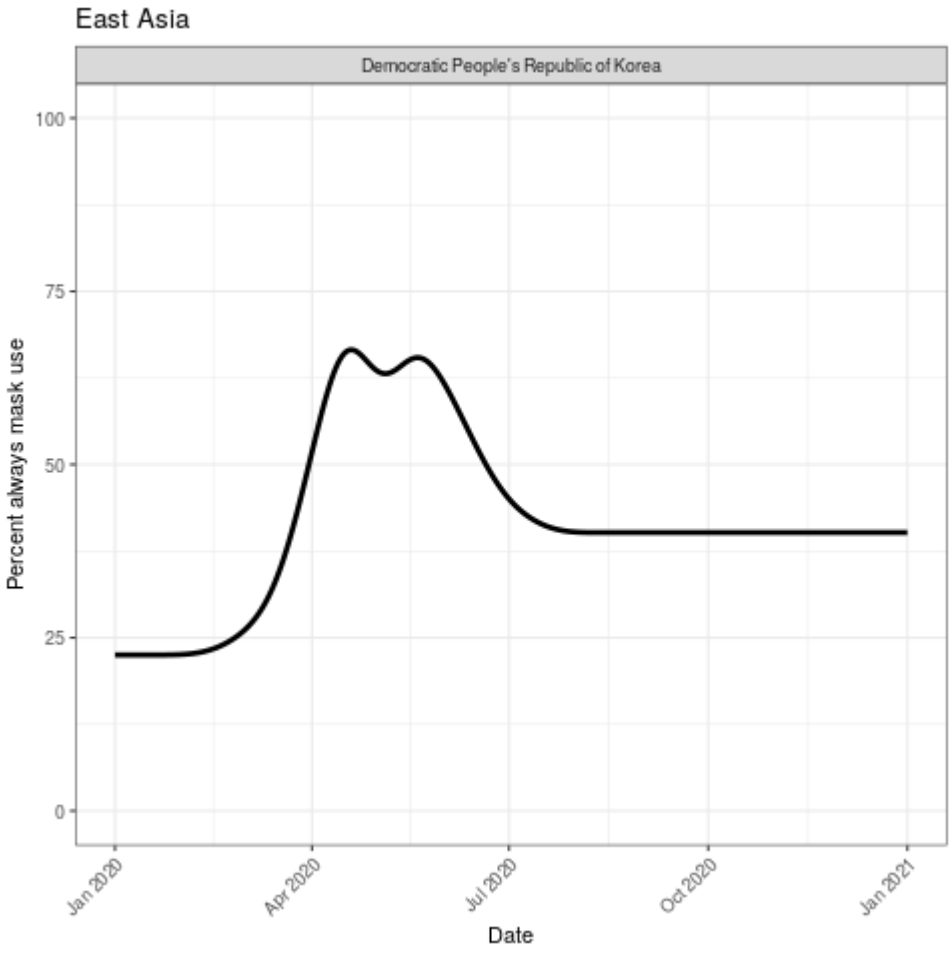

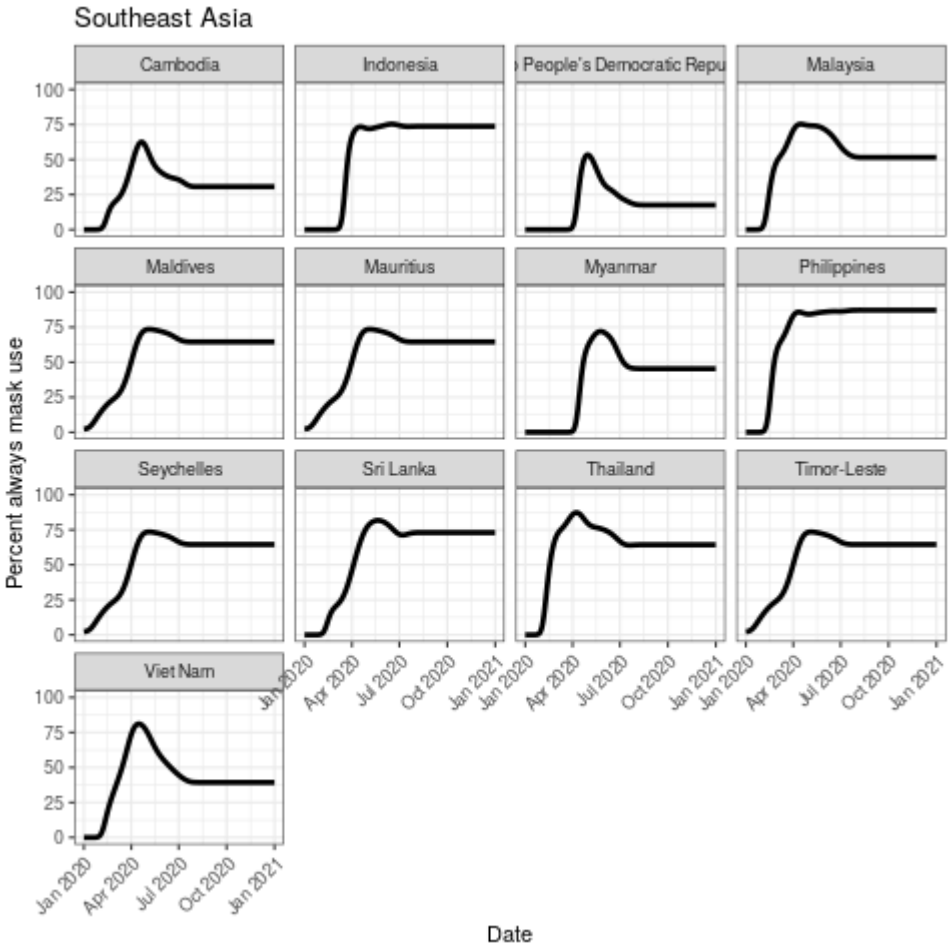
Southeast Asia
Cambodia
Indonesia
People's Democratic Repu
Malaysia
Maldives
Mauritius
Myanmar
Philippines
Seychelles
Sri Lanka
Thailand
Timor-Leste
Viet Nam
Percent always mask use
100
75
50
25
0
Jan 2020
Apr 2020
Jul 2020
Oct 2020
Jan 2021
Date

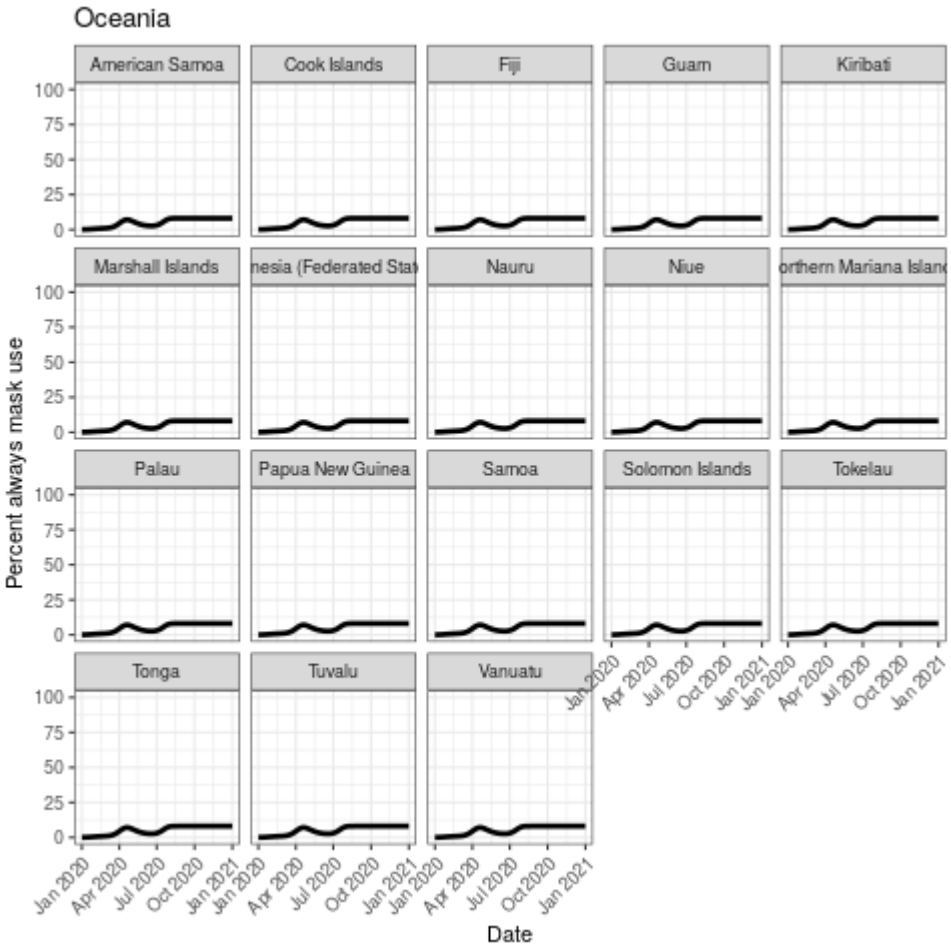
Oceania
American Samoa
Cook Islands
Fiji
Guam
Kiribati
Marshall Islands
Nauru
Niue
Palau
Papua New Guinea
Samoa
Solomon Islands
Tokelau
Tonga
Tuvalu
Vanuatu
Percent always mask use
0
25
50
75
100
Jan 2020
Apr 2020
Jul 2020
Oct 2020
Jan 2021
Date

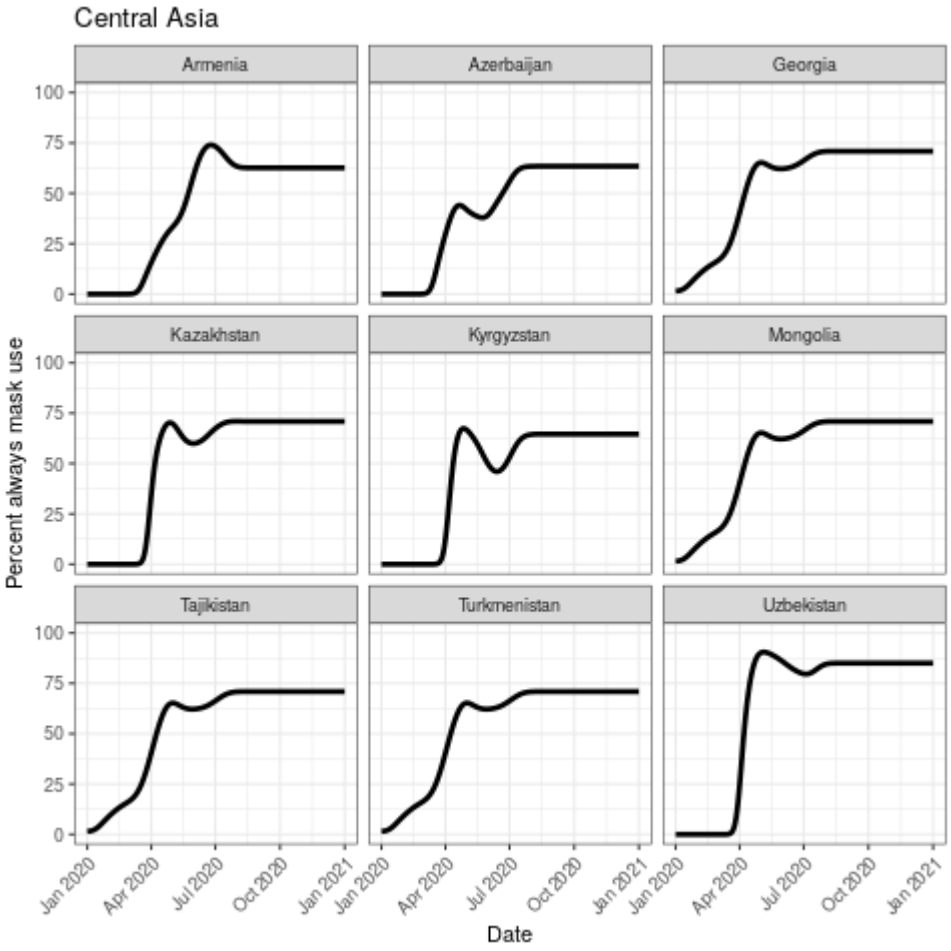
Central Asia
Armenia
Azerbaijan
Georgia
Kazakhstan
Kyrgyzstan
Mongolia
Tajikistan
Turkmenistan
Uzbekistan
Percent always mask use
0
25
50
75
100
Jan 2020
Apr 2020
Jul 2020
Oct 2020
Jan 2021
Date

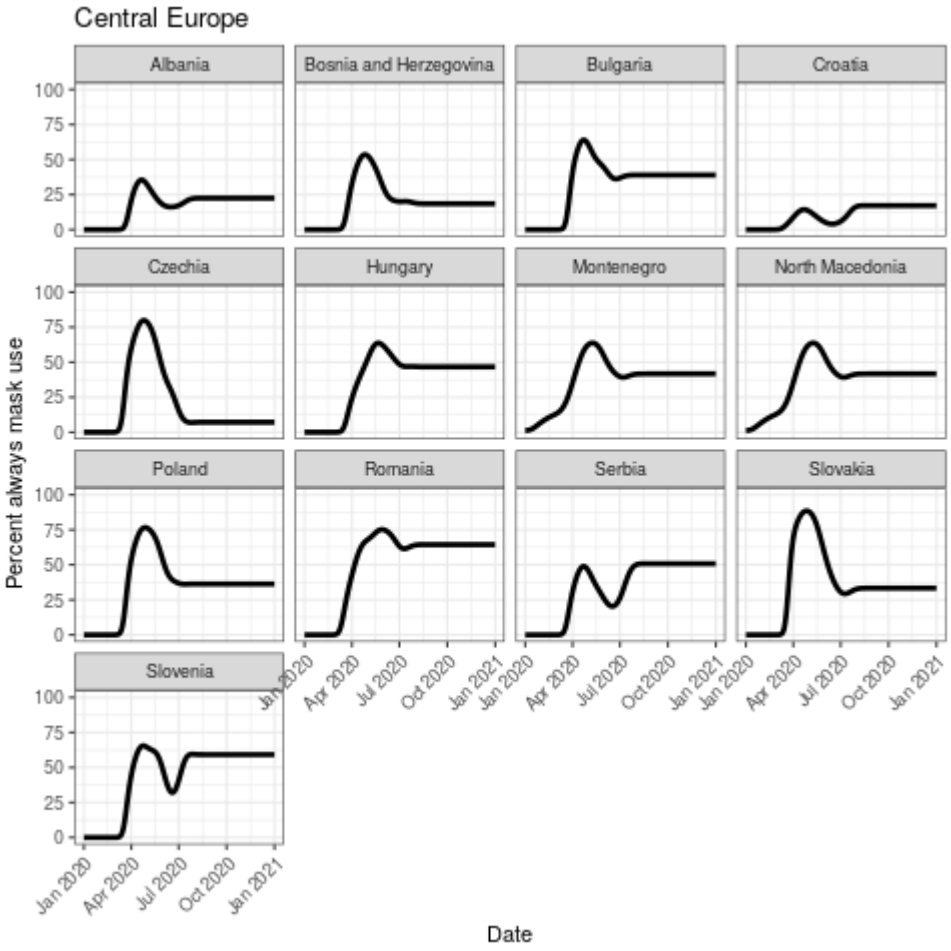
Central Europe
Albania
Bosnia and Herzegovina
Bulgaria
Croatia
Czechia
Hungary
Montenegro
North Macedonia
Poland
Romania
Serbia
Slovakia
Slovenia
Percent always mask use
0
25
50
75
100
Jan 2020
Apr 2020
Jul 2020
Oct 2020
Jan 2021
Date

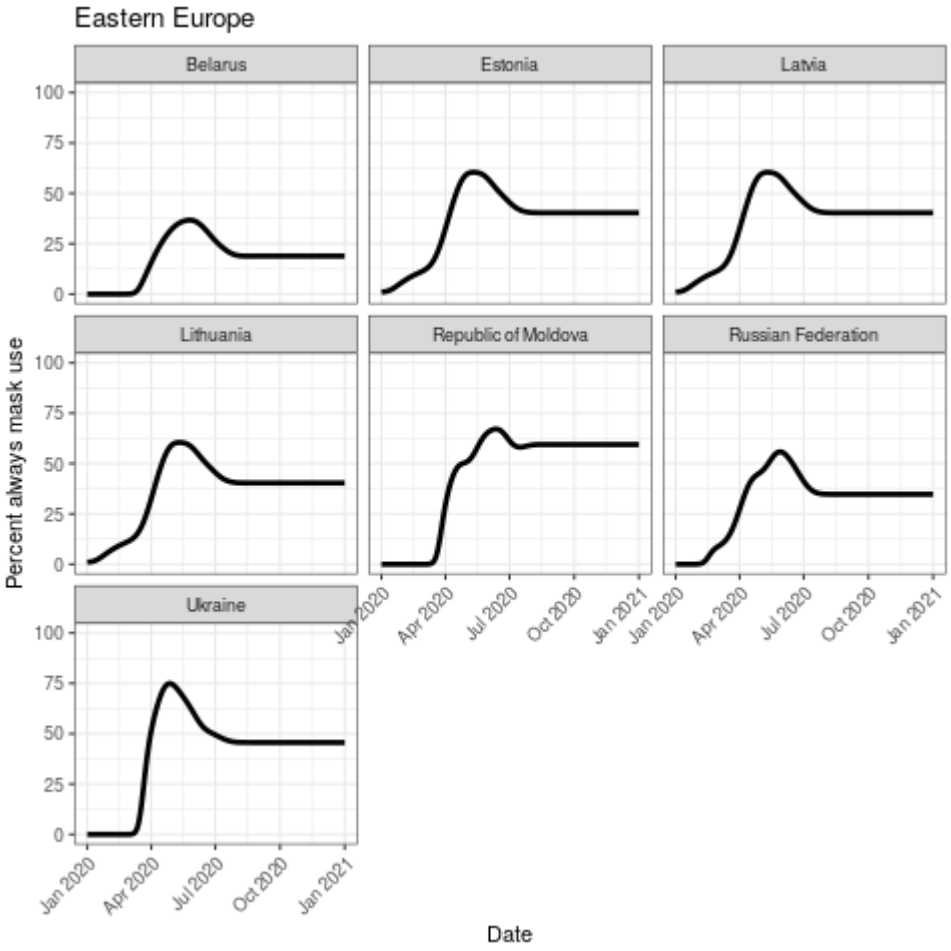
Eastern Europe
Belarus
Estonia
Latvia
Lithuania
Republic of Moldova
Russian Federation
Ukraine
Percent always mask use
100
75
50
25
0
Jan 2020
Apr 2020
Jul 2020
Oct 2020
Jan 2021
Date

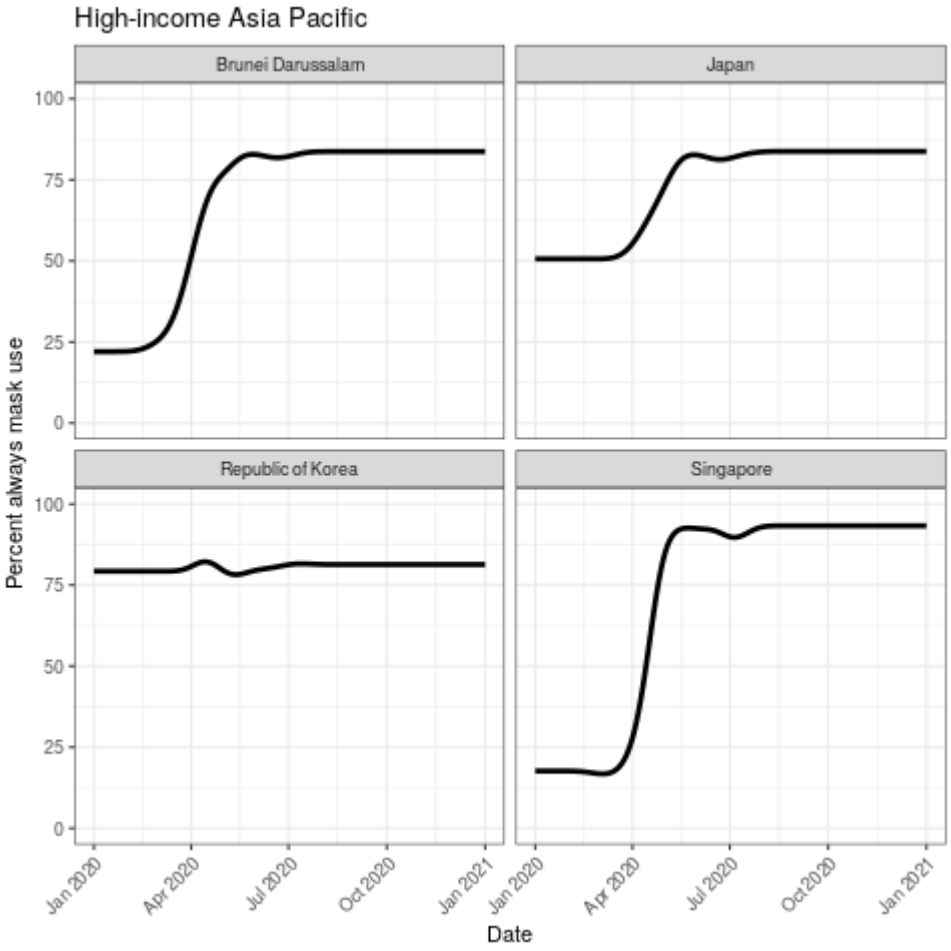
High-income Asia Pacific
Brunei Darussalam
Japan
Republic of Korea
Singapore
Percent always mask use
100
75
50
25
0
Jan 2020
Apr 2020
Jul 2020
Oct 2020
Jan 2021
Date

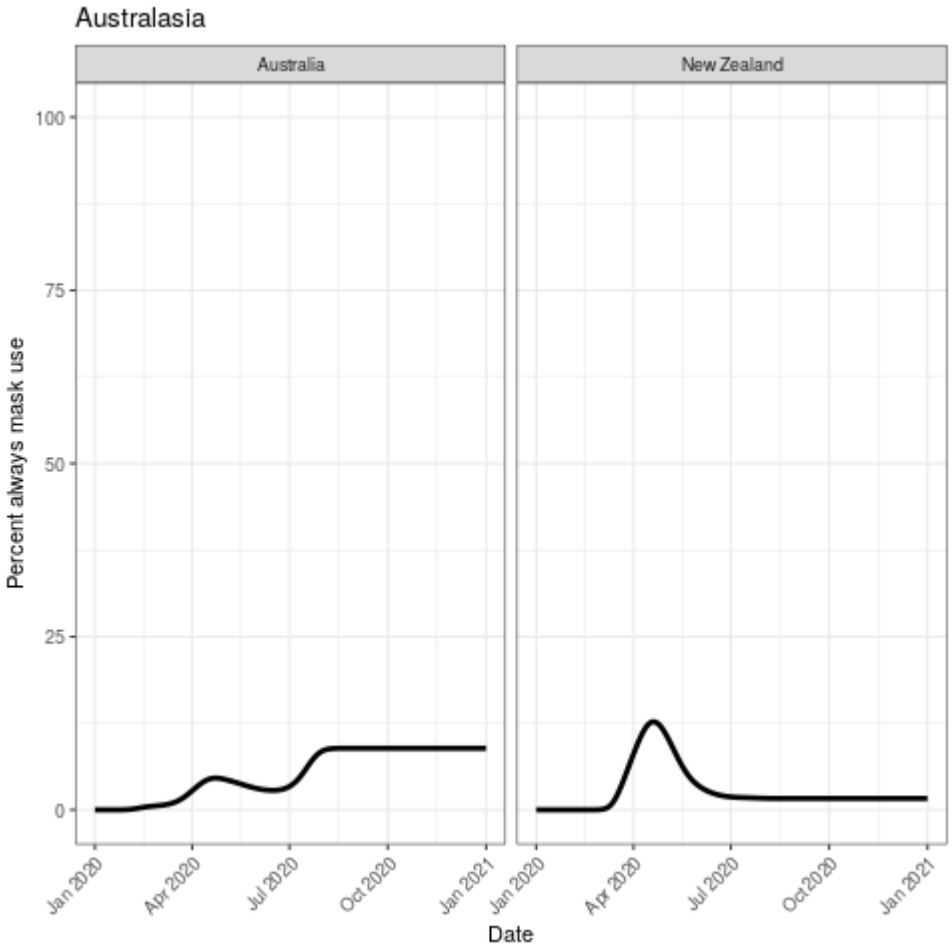
Australasia
Australia
New Zealand
Percent always mask use
100
75
50
25
0
Jan 2020
Apr 2020
Jul 2020
Oct 2020
Jan 2021
Date

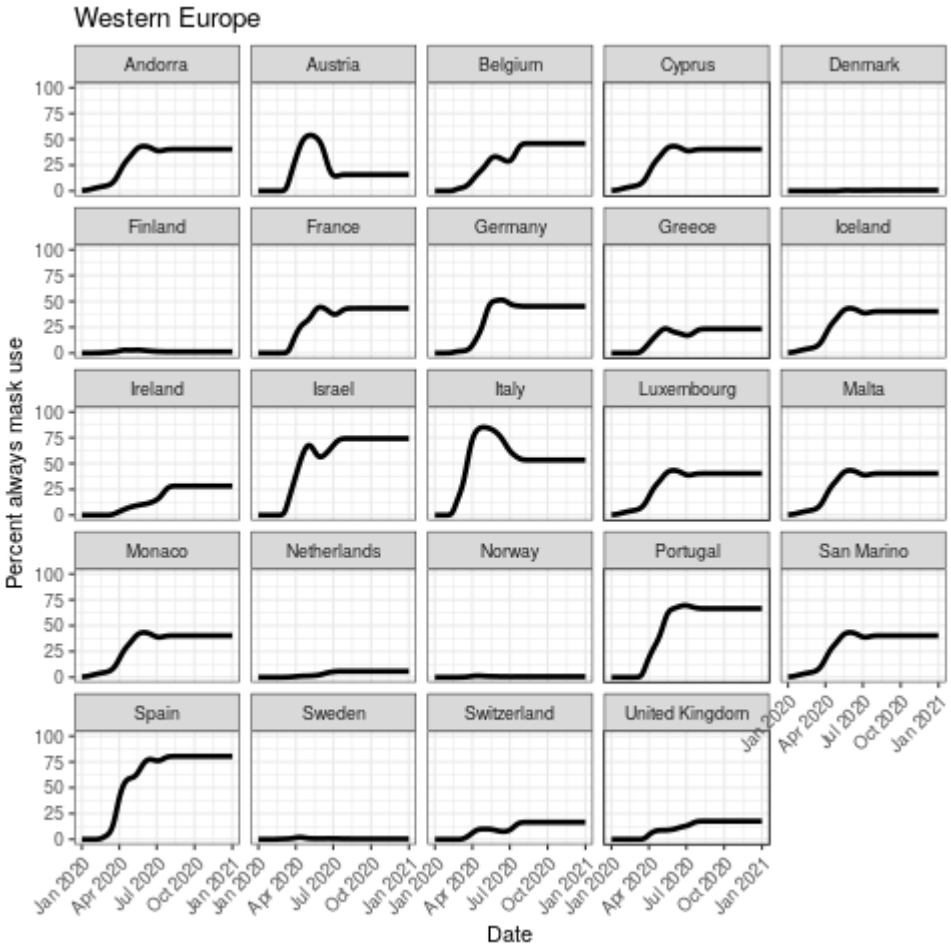
Western Europe
Andorra
Austria
Belgium
Cyprus
Denmark
Finland
France
Germany
Greece
Iceland
Ireland
Israel
Italy
Luxembourg
Malta
Monaco
Netherlands
Norway
Portugal
San Marino
Spain
Sweden
Switzerland
United Kingdom
Percent always mask use
0
25
50
75
100
Jan 2020
Apr 2020
Jul 2020
Oct 2020
Jan 2021
Date

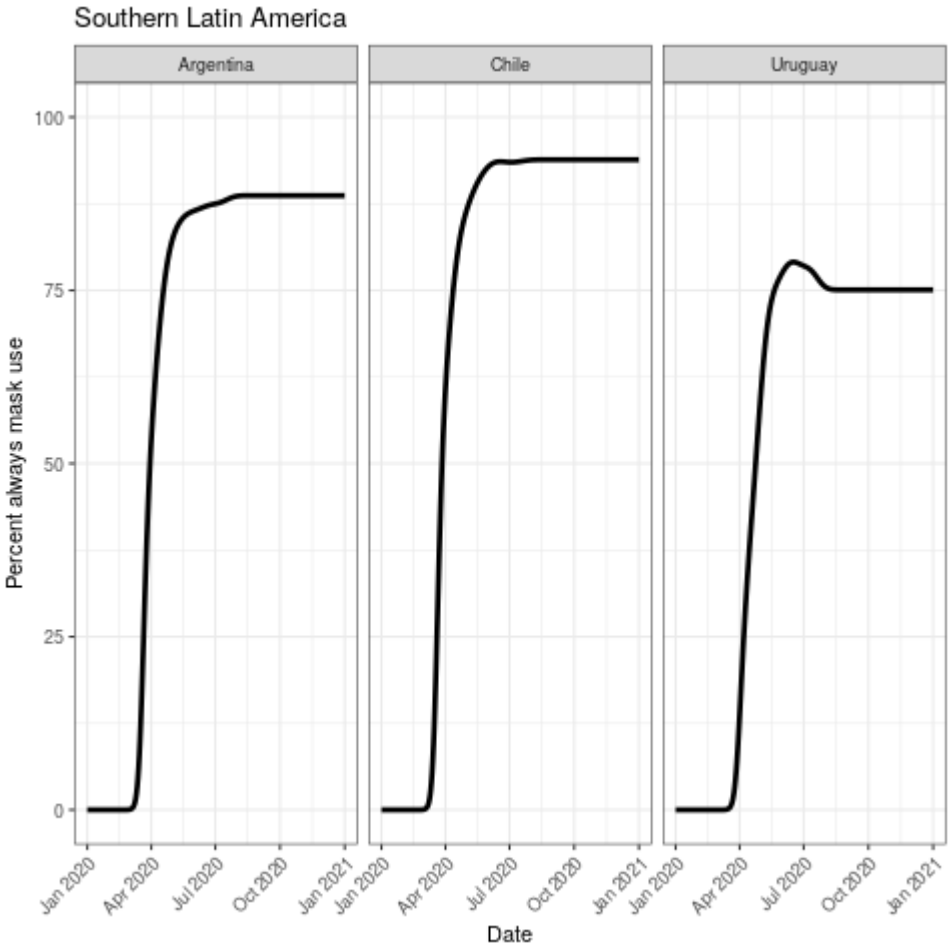
Southern Latin America
Argentina
Chile
Uruguay
Percent always mask use
100
75
50
25
0
Jan 2020
Apr 2020
Jul 2020
Oct 2020
Jan 2021
Date

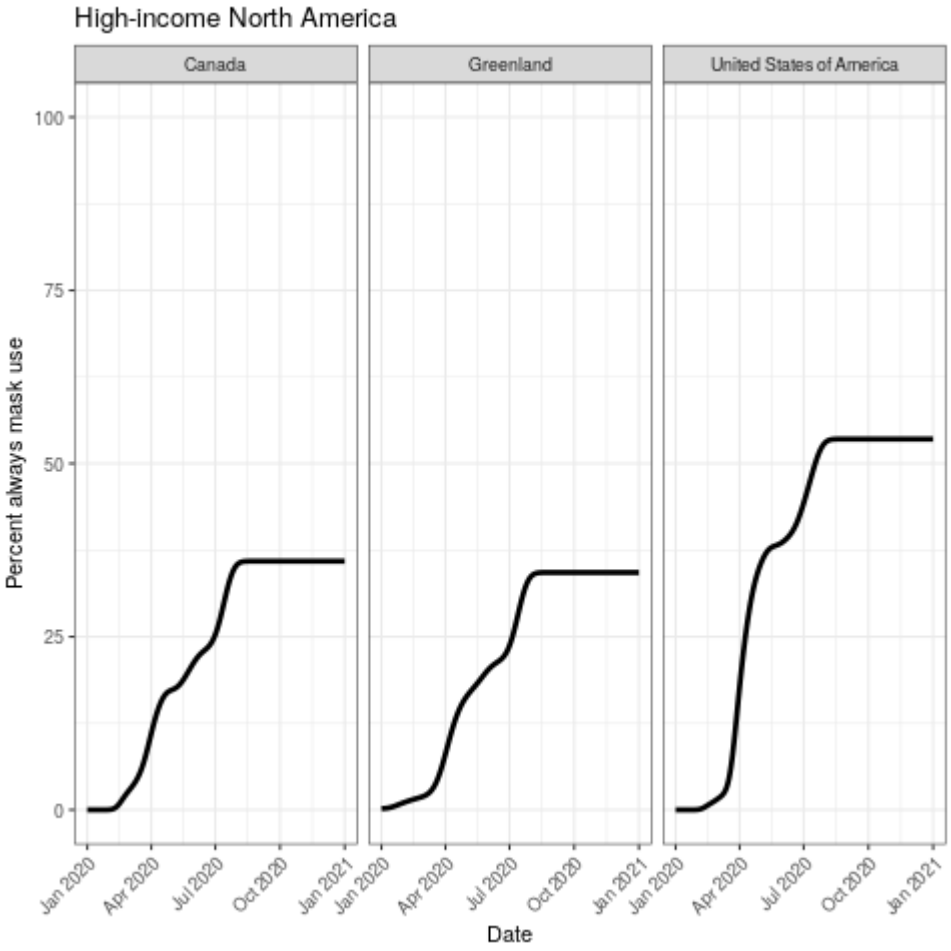
High-income North America
Canada
Greenland
United States of America
Percent always mask use
100
75
50
25
0
Jan 2020
Apr 2020
Jul 2020
Oct 2020
Jan 2021
Date

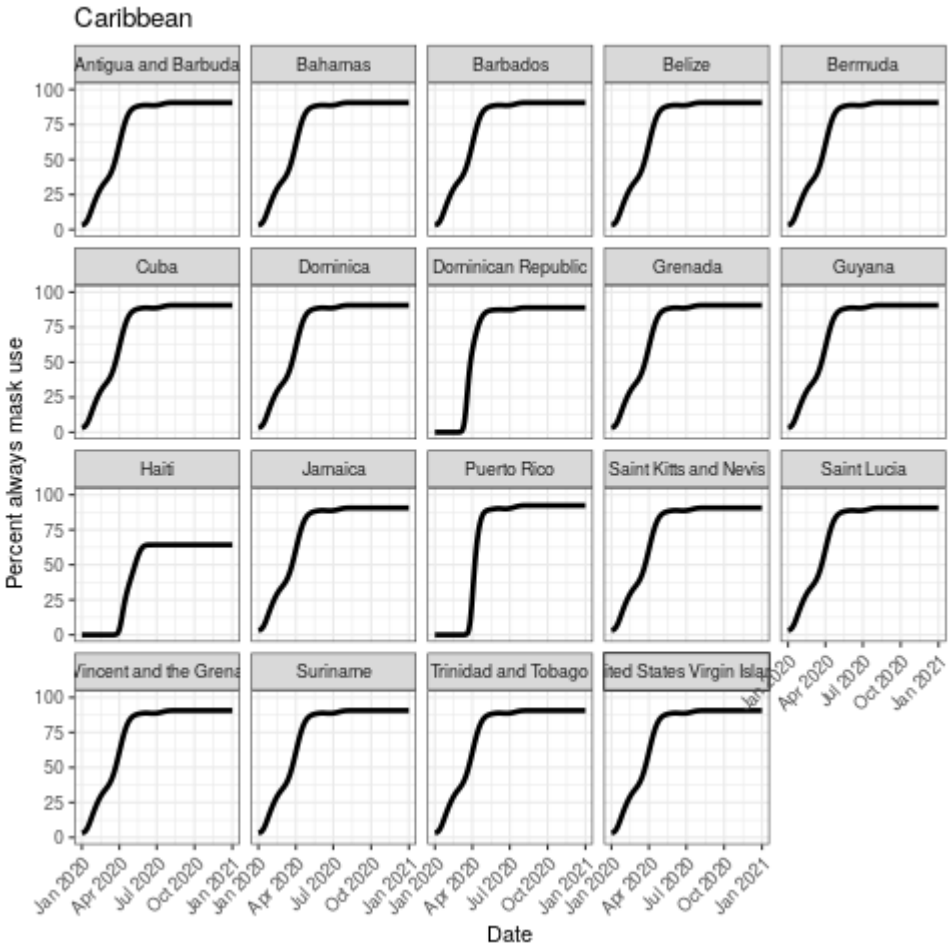
Caribbean
Antigua and Barbuda
Bahamas
Barbados
Belize
Bermuda
Cuba
Dominica
Dominican Republic
Grenada
Guyana
Haiti
Jamaica
Puerto Rico
Saint Kitts and Nevis
Saint Lucia
Vincent and the Grena
Suriname
Trinidad and Tobago
ited States Virgin Isla
Percent always mask use
0
25
50
75
100
Jan 2020
Apr 2020
Jul 2020
Oct 2020
Jan 2021
Date

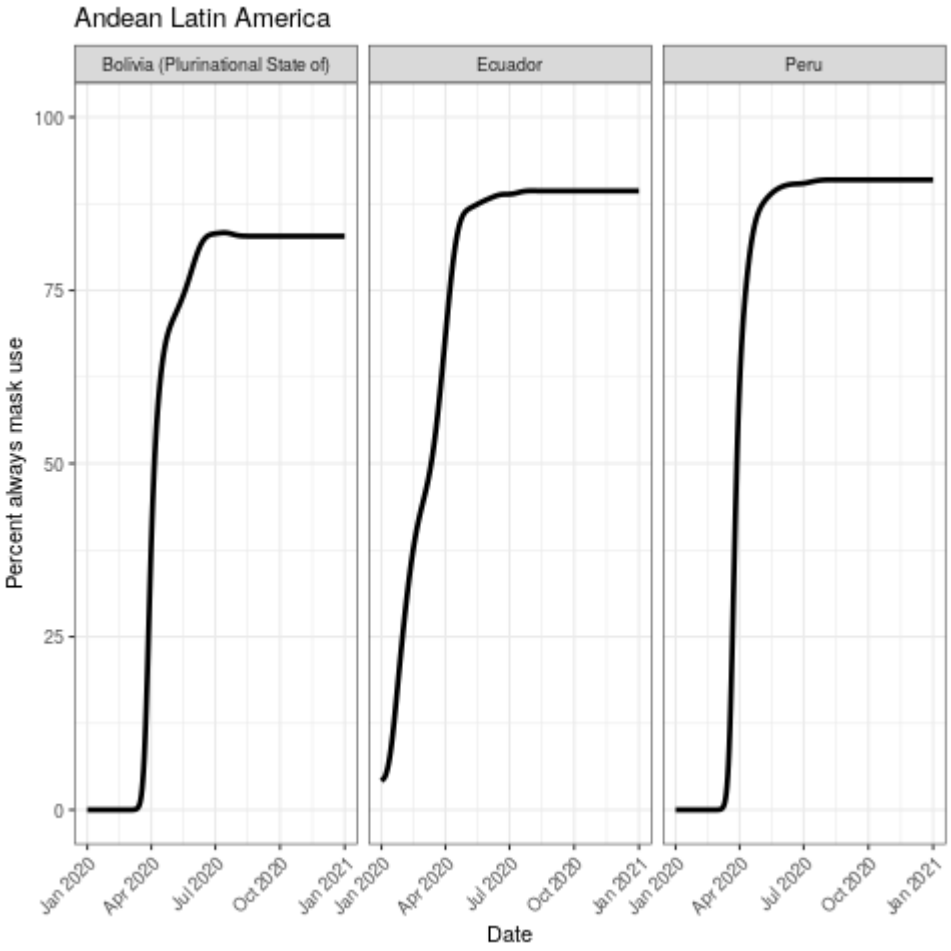
Andean Latin America
Bolivia (Plurinational State of)
Ecuador
Peru
Percent always mask use
100
75
50
25
0
Jan 2020
Apr 2020
Jul 2020
Oct 2020
Jan 2021
Date

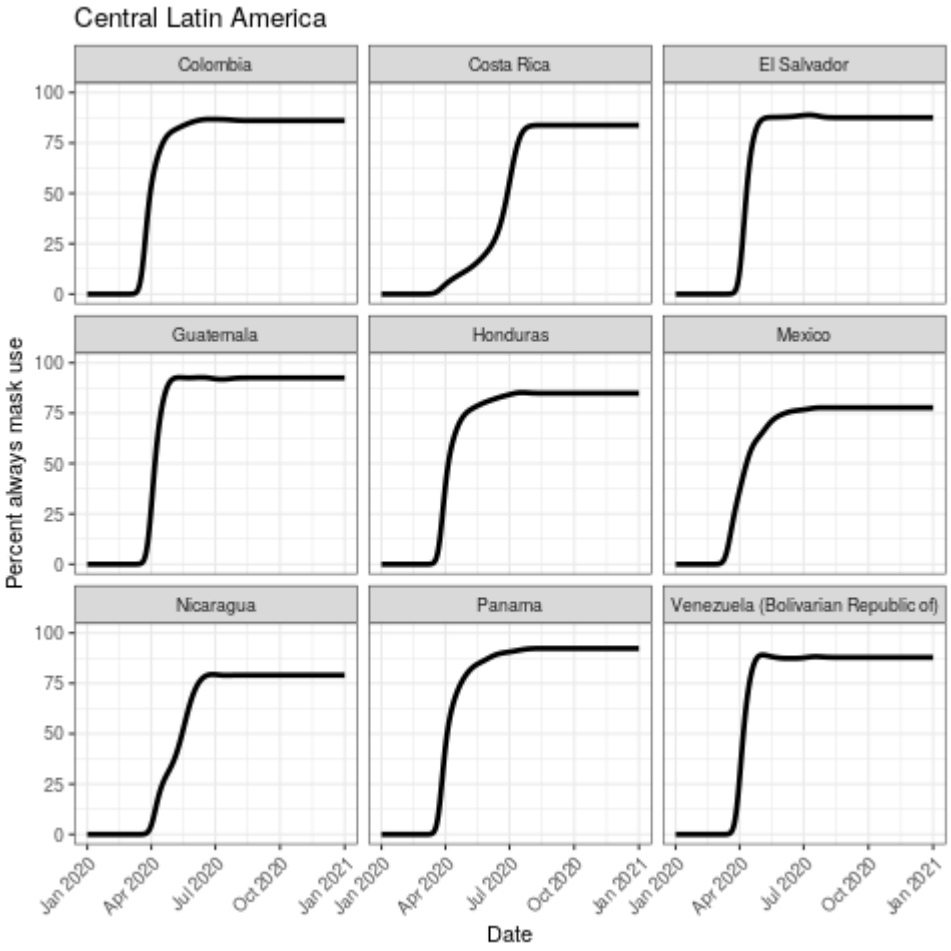
Central Latin America
Colombia
Costa Rica
El Salvador
Guatemala
Honduras
Mexico
Nicaragua
Panama
Venezuela (Bolivarian Republic of)
Percent always mask use
100
75
50
25
0
Jan 2020
Apr 2020
Jul 2020
Oct 2020
Jan 2021
Date

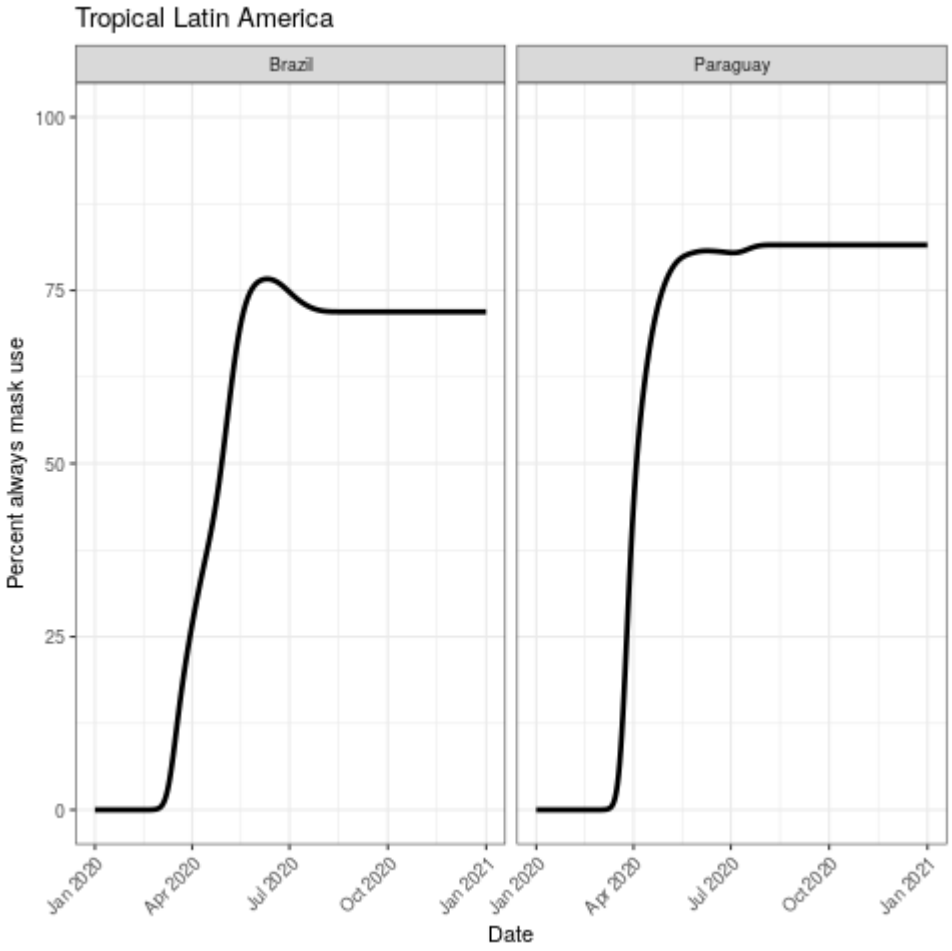
Tropical Latin America
Brazil
Paraguay
Percent always mask use
100
75
50
25
0
Jan 2020
Apr 2020
Jul 2020
Oct 2020
Jan 2021
Date

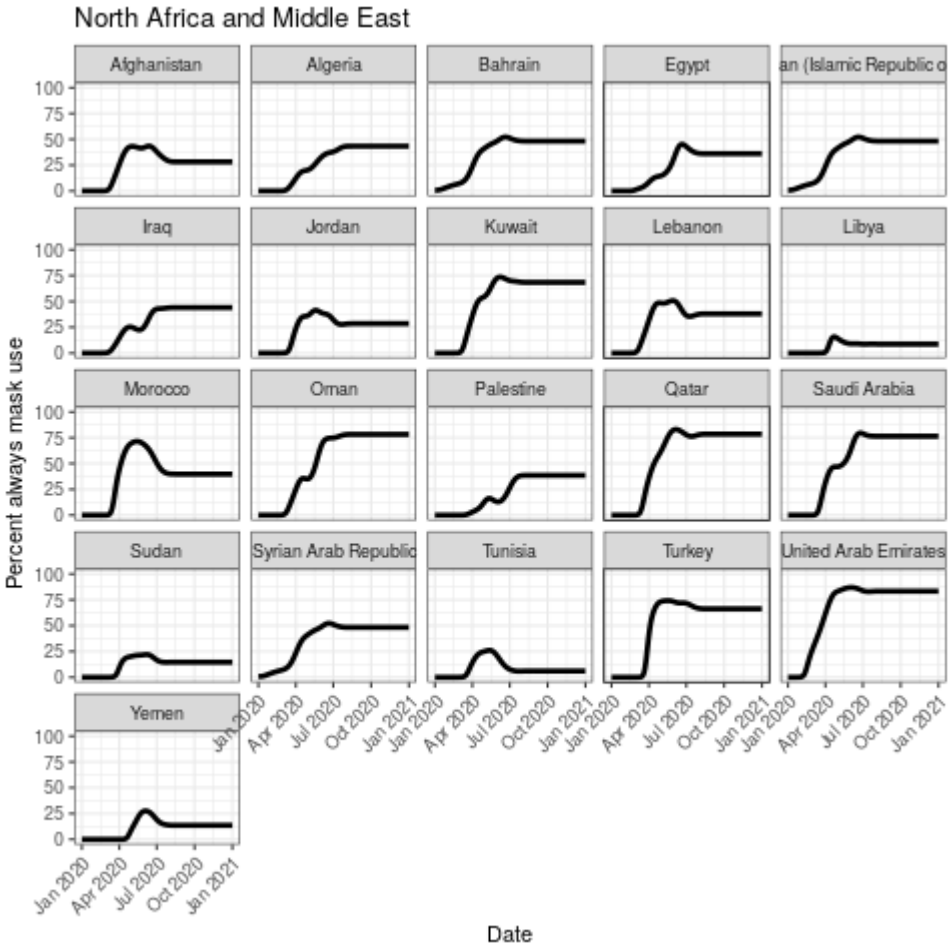
North Africa and Middle East
Afghanistan
Algeria
Bahrain
Egypt
an (Islamic Republic o
Iraq
Jordan
Kuwait
Lebanon
Libya
Morocco
Oman
Palestine
Qatar
Saudi Arabia
Sudan
Syrian Arab Republic
Tunisia
Turkey
United Arab Emirates
Yemen
Percent always mask use
100
75
50
25
0
Jan 2020
Apr 2020
Jul 2020
Oct 2020
Jan 2021
Date

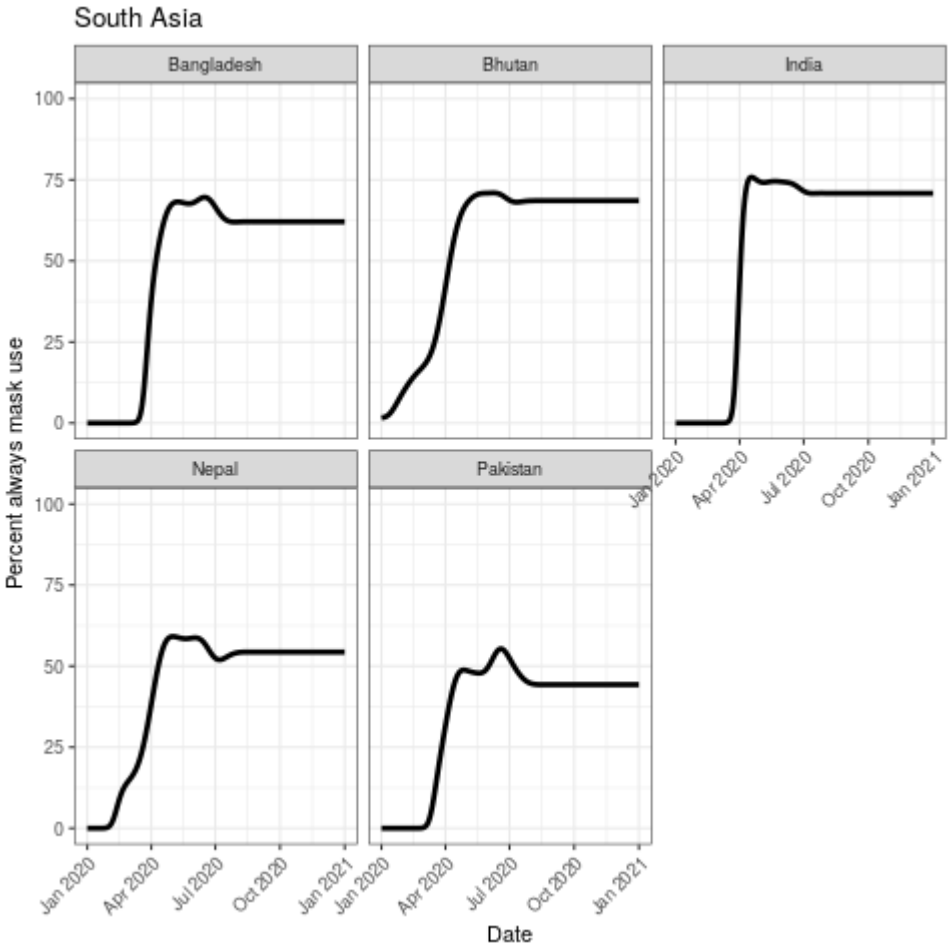
South Asia
Bangladesh
Bhutan
India
Nepal
Pakistan
Percent always mask use
100
75
50
25
0
Jan 2020
Apr 2020
Jul 2020
Oct 2020
Jan 2021
Date

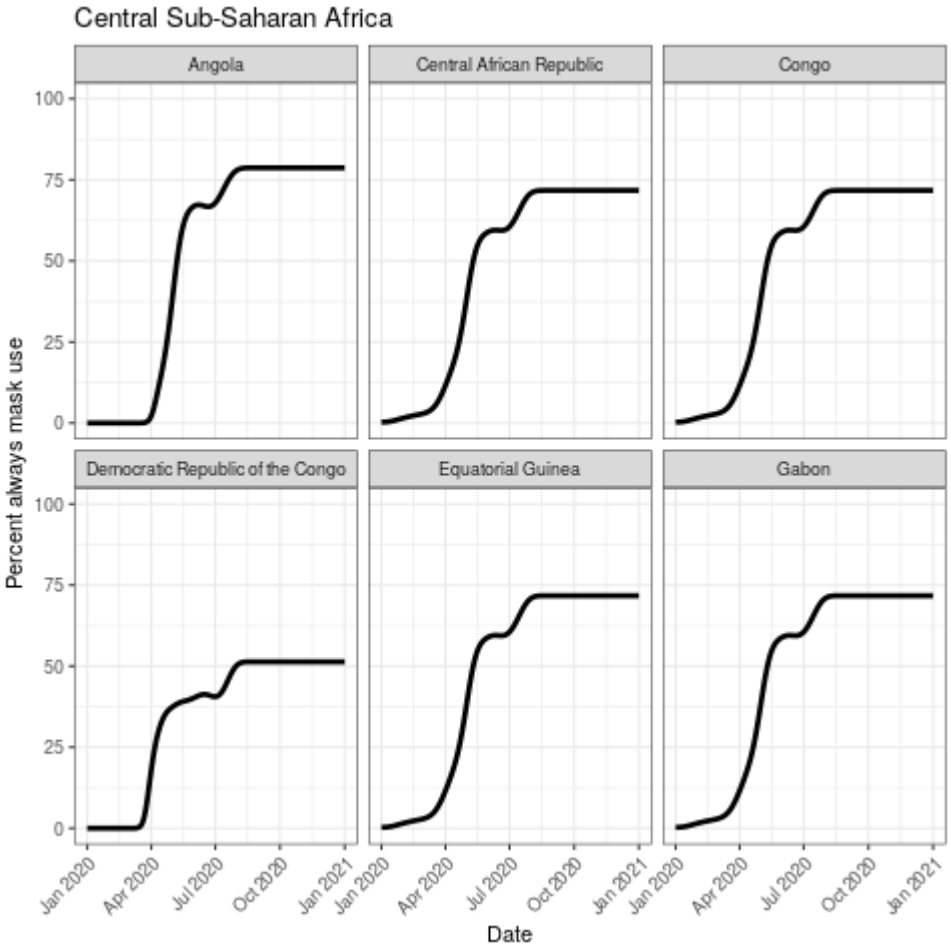
Central Sub-Saharan Africa
Angola
Central African Republic
Congo
Democratic Republic of the Congo
Equatorial Guinea
Gabon
Percent always mask use
100
75
50
25
0
Jan 2020
Apr 2020
Jul 2020
Oct 2020
Jan 2021
Date

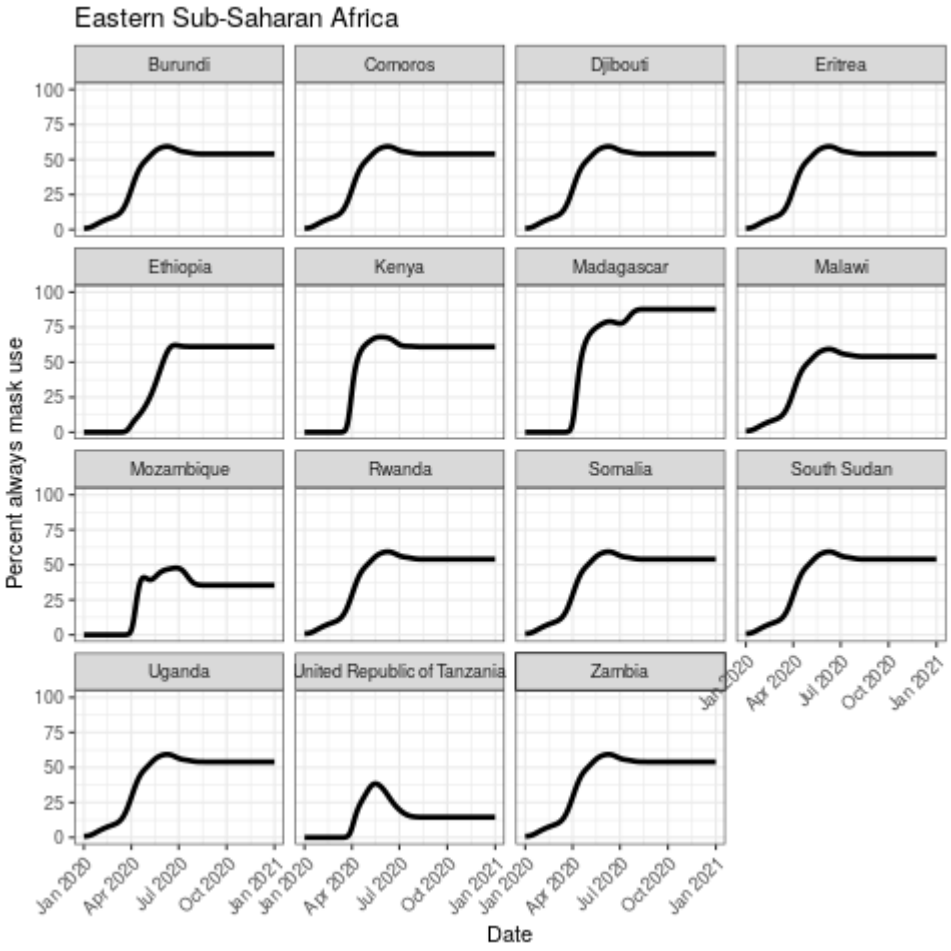
Eastern Sub-Saharan Africa
Burundi
Comoros
Djibouti
Eritrea
Ethiopia
Kenya
Madagascar
Malawi
Mozambique
Rwanda
Somalia
South Sudan
Uganda
United Republic of Tanzania
Zambia
Percent always mask use
0
25
50
75
100
Jan 2020
Apr 2020
Jul 2020
Oct 2020
Jan 2021
Date

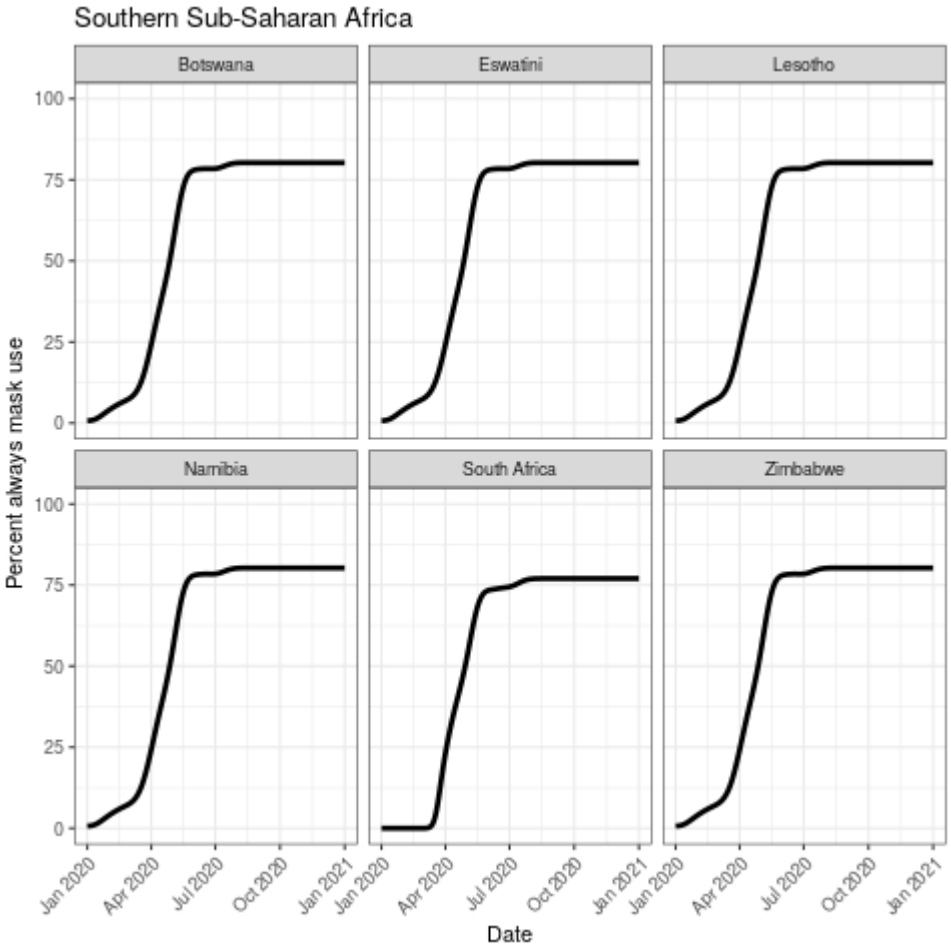
Southern Sub-Saharan Africa
Botswana
Eswatini
Lesotho
Namibia
South Africa
Zimbabwe
Percent always mask use
100
75
50
25
0
Jan 2020
Apr 2020
Jul 2020
Oct 2020
Jan 2021
Date

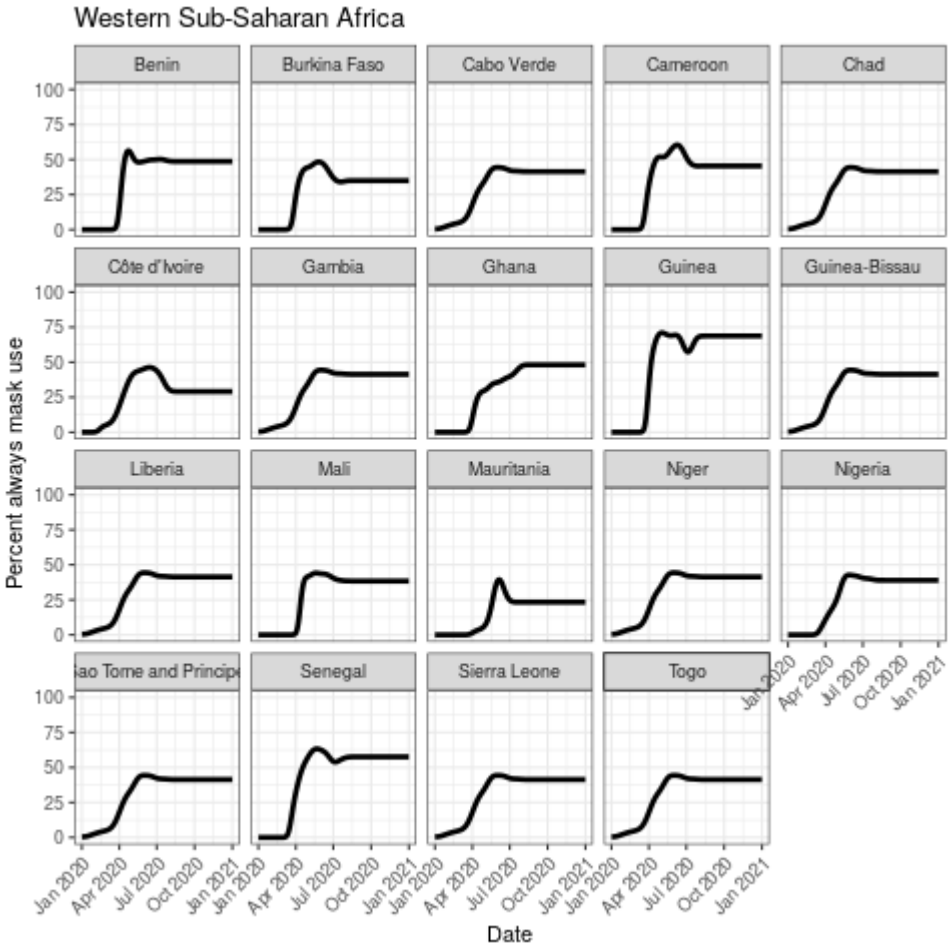
Western Sub-Saharan Africa
Benin
Burkina Faso
Cabo Verde
Cameroon
Chad
Côte d'Ivoire
Gambia
Ghana
Guinea
Guinea-Bissau
Liberia
Mali
Mauritania
Niger
Nigeria
ao Tome and Princip
Senegal
Sierra Leone
Togo
Percent always mask use
0
25
50
75
100
Jan 2020
Apr 2020
Jul 2020
Oct 2020
Jan 2021
Date

Section 3. IHME's COVID-19 Projections Modeling Framework.

The details of IHME's COVID-19 Projections Modeling Framework are described in detail elsewhere and can be found here: https://doi.org/10.1101/2020.07.12.20151191

In this section we provide more information on the components of the model that are most related to the analysis presented in this manuscript.

Modeling past deaths using random knot combination splines (RKCS)

In order to derive infections from deaths and the infection fatality rate (see below) for use in the transmission model, we first develop a series of spline regressions using IHME's customized meta-regression tool MR-BRT. MR-BRT ("meta-regression—Bayesian, regularized, trimmed") is a trimmed constrained mixed-effects model that provides an easy interface for formulating and solving common linear and nonlinear mixed effects models. It is open source, and its core computational kernel uses the mixed effects package LimeTr (https://github.com/zhengp0/limetr) and the spline package XSpline (https://github.com/zhengp0/xspline). For the statistical models and algorithmic features underlying MR-BRT, a published technical report is available[1].

The spline regressions obtained from MR-BRT smooth the trend in reported deaths and leverage patterns in reported case and hospital admissions data where available to make short term (8-day) forecasts of deaths. We use MR-BRT functionality that allows the user to specify a number of potential knot combinations to be randomly generated and runs separate models for each combination, which are then evaluated for performance and combined using those scores to create a weighted composite of the sub-models. We use 50 combinations in each of the subsequently described model stages, which are run separately by location.

Data and model overview

Deaths and cases by day were available for every location; hospital admissions data were also available for 27 states. Before merging with deaths for modelling we account for the lag between onset of symptoms and death based on the Global Line List (https://github.com/beoutbreakprepared/nCoV2019) by shifting dates for these measures to be 8 days later than reporting date.

Deaths from reported cases and hospitalizations

In the first stage we model the log cumulative death rate with either the log cumulative case rate or the log cumulative hospital admission rate as independent variables. Where data for both of the independent variables are available, separate models are run for each measure. We use a cubic spline with six knots, but with the left- and right-most intervals forced to be linear rather than cubic. We constrain the curve such that deaths monotonically increase along with cases/hospitalizations. Because of the shift window, we have 8 days of case and hospitalization data that extend past the last day of death data used to fit the model – by linearly extrapolating the tail of the fitted curve, we produce 8-day projections of deaths in addition to our in-sample fit. These estimates capture the trend in cases or hospitalizations while effectively accounting for changing case- and hospitalization-fatality ratios due to variation in exogenous factors such as age pattern of cases and testing rates.

Fitting final deaths curve with uncertainty

Using deaths estimated through cases and hospitalizations from the model described above, in addition to observed deaths, we then fit a second stage model using all three sources with time (in days) as the

independent variable. For this model, we run with two alternative dependent variable transformations – log cumulative deaths and log daily deaths, with an offset of 0.01 deaths per capita. While the latter is most effective at closely following the daily time trend, it can perform poorly in settings where there are few deaths due to overdispersion. As such, we use an algorithm that creates a linear combination of the two predictions where the weight given to the daily model result is equal to the total number of deaths in a location divided by 50 (capped at 1), and the cumulative model result receives the remaining weight. This prevents an abrupt transition in modeling strategy that would occur were we to use a singular threshold. In the cumulative model, we use the same settings as the previous stage – cubic spline with 6 knots, linear tails, and constrained to be monotonically increasing with the independent variable (time, in this case). The daily model is identical but without the monotonicity constraint.

With the resultant curve, we calculate the robust standard error using residuals in log daily space and create 1000 independent samples around the mean of that curve for each day, making 1000 uncorrelated time series representative of the observed noise in the data. We refit the log daily deaths model to each of these time series, giving us smooth estimates of death with uncertainty for the full range of dates with observed deaths and extending out to an 8-day forecasts.

Estimating infections from deaths

Conditioning on the death draws and the Infection Fatality Rate (IFR) and age-specific mortality rate (MR) (see below), daily infections are inferred by stratifying all-age deaths into age-specific deaths, using the age-specific IFR to determine the number of infections that would have led to this quantity of age-deaths, and then backshifting the infections in time to account for the lag between infection and deaths.

For each of the $j \in 1, \ldots, 1000$ cumulative death draws time-series, CD^j , one infection-to-death lag, l^j is randomly sampled from a discrete uniform distribution on 17 to 21 days.

For each lowest-level location, loc:

1. Daily deaths time-series, $DD^j(loc)$, are generated by differencing the cumulative deaths time-series, $CD^j(loc)$.
2. The mortality probabilities, $MP_{ageBin_i}(loc)$, for an individual in this location belonging to each 5-year age bins, $ageBin_i$, is calculated:
$$MP_{ageBin_i}(loc) = \frac{MR_{ageBin_i}(loc) \times Pop_{ageBin_i}(loc)}{\Sigma_i (MR_{ageBin_i}(loc) \times Pop_{ageBin_i}(loc)},$$
where $Pop_{ageBin_i}(loc)$, is the total population for that $ageBin_i$ at loc. If this is not available, we resort to using the parent location's population.
3. The expected age-specific daily deaths time-series, $DD^j_{ageBin_i}(loc)$, is calculated by stratifying the all-age deaths using the age-specific mortality probabilities, $MP_{ageBin_i}(loc)$:
$$DD^j_{ageBin_i}(loc) = MP_{ageBin_i}(loc) \times DD^j(loc).$$
4. The expected age-specific daily infections time-series, $DI^j_{ageBin_i}(loc)$, are calculated from the age-specific IFR and daily deaths:
$$DI^j_{ageBin_i}(loc) = DD^j_{ageBin_i}(loc)/IFR_{ageBin_i}(loc)$$

5. The date of the infection time-series is taken to be the date of the death time series shifted back by l^j days.
6. The all-age daily infection time-series is prepared for the SEIR model by summing the infections across all age groups:

$$DI^j(loc) = \Sigma_i DI^j_{ageBin_i}(loc).$$

This process yields 1000 draws of daily new infections across all modeled locations.

$$MR_{ageBin_i}(loc)/\Sigma_i MR_{ageBin_i}(loc) A_D H: D_{A_D}$$

Intermediate quantity modeling

Mortality rate by age estimation

To determine the age-pattern of mortality, we assembled available data from multiple global locations. A continuous model relating age and mortality from which the average mortality for any discrete age bins can be aggregated. We assume a Poisson model for death counts and fit a monotonically increasing (shape-constrained) generalized additive model (SCAM) for mortality as a function of age, using the medians of each of the N_{loc} age bins, $ageBin_i^M(loc)$:

$$\log\big(E[MortalityRate_{AgeBin_i(loc)}(loc)]\big) = \log(Pop_{AgeBin_i(loc)}(loc) + f_1\left(ageBin_i^M(loc)\right) + \cdots + f_k\left(ageBin_i^M(loc)\right),$$

where $f_.()$ are monotonically increasing P-splines, and k, the number of bases functions, is between 6 and 8 and tuned for different locations. This yields continuous mortality rates by age: $MR_a(loc)$.

Similarly, assuming a Poisson model, we fit a generalized additive model (GAM) to population as a function of age, using the age groups specified in the mortality data for each location:

$$\log\big(E[Pop_{AgeBin_i(loc)}(loc)]\big) = g_1\left(ageBin_i^M(loc)\right) + \cdots + g_k\left(ageBin_i^M(loc)\right),$$

where $g_.()$ are penalized thin-plate regression splines, and k, the number of bases functions, is between 6 and 8 and tuned for different locations. This yields continuous population by age: $pop_a(loc)$.

The estimated continuous mortality rate curves are then aggregated using population weights to the pre-determined $ageBin(CDC)$s:

$$MR_{ageBin_i(CDC)}(loc) = \frac{\sum_{a \in ageBin_i(CDC)} MR_a(loc) * pop_a(loc)}{\sum_{a \in ageBin_i(CDC)} pop_a(loc)}.$$

Infection fatality ratio

We estimated the ratio of deaths to infections using random effects meta-analysis, with random intercepts by location and a spline to estimate the non-linear effect of age. The spline

method allows for the estimation of a continuous age effect from observations recorded as age groups. In addition to data on the quantity of interest – deaths divided by infections – the model incorporated data on deaths divided by population to better estimate the age trend. The final estimate comes from the location with the lowest estimated IFR, New Zealand. We chose this approach because asymptomatic infections are often not detected, so we expect that reported IFRs are systematically higher than the true IFR. The Diamond Princess cruise ship was included among the locations used for this analysis.

Infection to death duration

To estimate the time from infection to death, we brought together two distinct sources of information: published studies of time from infection to symptoms and individual patient data on time from symptom onset to death. Due to a paucity of data on the time from infection to symptom onset, we used the median time reported from a single source (5.1 days) for the first part of this duration and added it to a distribution for the second derived by pooling data from the Global Line List (https://github.com/beoutbreakprepared/nCoV2019); Ohio, USA (https://coronavirus.ohio.gov/wps/portal/gov/covid-19/dashboards); Rio de Janeiro State, Brazil (http://painel.saude.rj.gov.br/monitoramento/covid19.html); Ceara State, Brazil (https://indicadores.integrasus.saude.ce.gov.br/indicadores/indicadores-coronavirus/coronavirus-ceara); and Mexico. This pooled dataset included data on 5,125 individuals, with a median time from onset of symptoms to death of 11 days. Informed by this, we use a uniform distribution over 17 to 21 days of lag between infection and death.

Hospitalizations to death ratio

To determine hospitalization, we use cumulative hospital to cumulative deaths ratios estimated directly from hospitalization and mortality data in the US and Europe through April 2020. We assembled data on COVID-19 hospitalizations from a number of countries and US states. We analyzed hospitalization to death ratios using random effects meta-analysis. We used the location-specific random effect in the estimate for locations with data. In the absence of data we used the corresponding pooled effect for other countries.

As the hospitalization to death ratios are for all-ages only, to estimate the age-pattern of the hospitalization to death ratio, we used the age distribution of hospitalization to death ($H{:}\,D$) in the US to estimate the age-distribution for other countries and states:

$$H{:}\,D_{ageBin}(\mathrm{loc}) = \frac{H{:}\,D_{ageBin}(US) \ * H{:}\,D_{allAge}(loc)}{(H{:}\,D_{ageBin}(US) * D_{ageBin}(loc))/D_{allAge}(loc)}$$

COVID-19 SEIR model construction for each location

Overview

The primary model for estimating future infections and deaths is a mechanistic compartmental model. Specifically, the fraction of each location's population that is susceptible (S), infected but not infectious (exposed, E), infectious (I_1, I_2), and recovered (R), forming an SEIR model. Temporal variations in past transmission intensity is captured through the time-varying parameter $\beta(t)$. The association between the time-varying transmission intensity and a number of covariates is assessed in a multivariate mixed effects regression across all locations simultaneously. Each of the covariates is then forecast into the future, with certain covariates forecast multiple times corresponding to unique future scenarios. The forecast covariate values and the fitted regression model are then used to estimate future transmission intensity; the future transmission intensity is then used in the SEIR framework to estimate future infections. Finally, reversing the process that estimated past infections from past deaths, future deaths are estimated from future infections.

SEIR-fit

Model formulation

To project the full time-series of deaths and infections to the future, we use a transmission model with the following compartments: susceptible, exposed, infected, and removed (SEIR). In particular, each location's population is tracked through the following system of differential equations:

$$\frac{dS}{dt} = -\beta(t)\frac{S(I_1 + I_2)^\alpha}{N}$$
$$\frac{dE}{dt} = \beta(t)\frac{S(I_1 + I_2)^\alpha}{N} - \sigma E$$
$$\frac{dI_1}{dt} = \sigma E - \gamma_1 I_1$$
$$\frac{dI_2}{dt} = \gamma_1 I_1 - \gamma_2 I_2$$
$$\frac{dR}{dt} = \gamma_2 I_2$$

where α represents a mixing coefficient to account for imperfect mixing within each location, σ is the rate at which infected individuals become infectious, γ_1 is the rate at which infectious people transition out of the pre-symptomatic phase, and γ_2 is the rate at which individuals recover. This model does not distinguish between symptomatic and asymptomatic infections but has two infectious compartments (I_1 and I_2) to allow for interventions that would avoid focus on those who could not be symptomatic. I_1 is thus the pre-symptomatic compartment.

R_c and the effective reproductive number $R_{eff}(t)$

In this section, we derive the time-varying basic reproductive number under control, $R_c(t)$, and the time-varying effective reproductive number, $R_{eff}(t)$. For a compartmental model with static coefficients, we can calculate the basic reproductive number as the largest singular value of the next generation operator

$$R_c = \lambda_{max}(FV^{-1})$$

where F is the Jacobian of the vector of appearance rates for compartments that actively possess the virus (E, I_1, and I_2 in our case), and $V = V^- + V^+$ is the Jacobian of the vector of transport rates of the individuals between these compartments. Both Jacobians are evaluated at the state of disease-free equilibrium (i.e., when $S = N$). The appearance and transport rate vectors for our SEIR model formulation are:

$$f = \begin{pmatrix} \beta \dfrac{S(I_1 + I_2)^{\alpha}}{N} \\ 0 \\ 0 \end{pmatrix}, \qquad v = \begin{pmatrix} \sigma E \\ \gamma_1 I_1 - \sigma E \\ \gamma_2 I_2 - \gamma_1 I_2 \end{pmatrix}.$$

We can then directly calculate the Jacobians at disease-free equilibrium:

$$F = \begin{pmatrix} 0 & \alpha\beta(I_1 + I_2)^{\alpha-1} & \alpha\beta(I_1 + I_2)^{\alpha-1} \\ 0 & 0 & 0 \\ 0 & 0 & 0 \end{pmatrix}$$

$$V = \begin{pmatrix} \sigma & 0 & 0 \\ -\sigma & \gamma_1 & 0 \\ 0 & -\gamma_1 & \gamma_2 \end{pmatrix} \Rightarrow V^{-1} = \begin{pmatrix} \dfrac{1}{\sigma} & 0 & 0 \\ \dfrac{1}{\gamma_1} & \dfrac{1}{\gamma_1} & 0 \\ \dfrac{1}{\gamma_2} & \dfrac{1}{\gamma_2} & \dfrac{1}{\gamma_2} \end{pmatrix}$$

Thus, the next generation operator is

$$FV^{-1} = \begin{pmatrix} \alpha\beta(I_1 + I_2)^{\alpha-1}\left(\frac{1}{\gamma_1} + \frac{1}{\gamma_2}\right) & \alpha\beta(I_1 + I_2)^{\alpha-1}\left(\frac{1}{\gamma_1} + \frac{1}{\gamma_2}\right) & \alpha\beta(I_1 + I_2)^{\alpha-1} \cdot \frac{1}{\gamma_2} \\ 0 & 0 & 0 \\ 0 & 0 & 0 \end{pmatrix}$$

which yields

$$R_c = \alpha\beta(I_1 + I_2)^{\alpha-1}\left(\frac{1}{\gamma_1} + \frac{1}{\gamma_2}\right)$$

Fitting $\beta(t)$

We denote the new daily infections output from the previous step as:

$$f(t) \approx \beta(t) S(I_1 + I_2)^{\alpha}$$

For each draw we take as constant the parameters governing the transmission dynamics other than $\beta(t)$ (i.e., α, σ, γ_1, and γ_2). These parameter values are drawn from distributions based on existing literature.

With a known $f(t)$, we can solve a single simple linear ODE to get $E(t)$:

$$\frac{dE}{dt} = -f(t) - \sigma E$$

This ODE can be solved in closed form using integrating factors, or numerically. In practice we use the 4th order Runge-Kutta method (RK-4). However, it is useful to solve it in 'closed form' using the integration factor approach. Defining

$$v(t) = \int \sigma dt = \sigma t,$$

we have the closed form solution

$$E(t) = \exp(-\sigma t) \int_0^t -f(\tau) \exp(\sigma\tau)\, d\tau + C \exp(-\sigma t), \quad C = E(0)$$

Having obtained $E(t)$, we repeat the process, solving for $I_1(t)$ and $I_2(t)$:

$$\begin{aligned}
&\frac{dI_1}{dt} + \gamma_1 I_1 = \sigma E(t) \\
&I_1(t) = \exp(-\gamma_1 t)\left(\int_0^t -f(\tau) \exp(\sigma\tau)\, d\tau\right) + I_1^0 \exp(-\gamma_1 t) \\
&= F_1(t) + I_1^0 \exp(-\gamma_1 t) \\
&\frac{dI_2}{dt} + \gamma_2 I_2 = \gamma_1 I_1(t) \\
&I_2(t) = \exp(-\gamma_2 t)\left(\int_0^t \gamma_1 I_1(\tau) \exp(\gamma_2\tau)\, d\tau\right) \\
&= \exp(-\gamma_2 t)\left(\int_0^t \gamma_1 (F_1(\tau) + I_1^0 \exp(-\gamma_1\tau))\ \exp(\gamma_2\tau)\, d\tau\right) \\
&= \exp(-\gamma_2 t)\left(\int_0^t \gamma_1\ F_1(\tau) \exp(\gamma_2\tau)\, d\tau\right) + \frac{I_1^0}{\gamma_2 - \gamma_1}(\exp(-\gamma_1 t) - \exp(-\gamma_2 t)) \\
&= F_2(t) + \frac{I_1^0}{\gamma_2 - \gamma_1}(\exp(-\gamma_1 t) - \exp(-\gamma_2 t))
\end{aligned}$$

where $E(t)$ is known when solving I_1, and then $I_1(t)$ is known when solving for I_2. While useful for formulation to think of the exact solutions, the integrals must still be solved numerically. We therefore solve all the differential equations using Runge-Kutta order 4. With $f(t)$ in hand, we also obtain $S(t)$ by simple integration and subtraction. Having solved for $S(t)$, $I_1(t)$, and $I_2(t)$, we then have:

$$\beta(t) = \frac{Nf(t)}{S(t)\big(I_1(t) + I_2(t)\big)^\alpha}$$

β regression

With $\beta_f(t)$ fit to the data, we next perform a linear regression using the open source mixed effects solver SLIME (https://github.com/zhengp0/SLIME) to determine the strength of the relationship between $\beta_f(t)$ and the various covariates. All covariates are assumed to have fixed effects while the intercept is allowed to vary by location. For location l, the regression is calculated as:

$$\ln(\beta_{p,l}) = \alpha_{0,l} + \boldsymbol{X}_l\boldsymbol{\alpha}$$

such that the mean squared error between $\beta_{p,l}$ and $\beta_{f,l}$ (our fit from the previous stage) is minimized by location l. $\alpha_{0,l}$ is the random intercept for location l, $\boldsymbol{X}_l$ is a matrix with a column for each covariate in the regression and a row for each day, and $\boldsymbol{\alpha}$ is the coefficient indicating the strength of the relationship between $\log\beta$ and the covariate. Several coefficients in the model are bounded as described in their corresponding sections, while others are only constrained by directional bounds. As noted in (previous sections), not all covariates are time varying. These non-time varying covariates are used to explain some of the location specific variance otherwise absorbed into the random intercept. Using the fitted α and the forecasted covariates, we produce, by draw, estimates of future transmission intensity $\beta_p(t)$.

β adjustments

To ensure continuity from our fitted β_f from SEIR-fit to the predicted β_F into the future, we shift the predicted β_p. Generally speaking, we shift β_p towards β_f by first ensuring that on the day of transition, say T, $\beta_F(T) = \beta_f(T)$. Then, over a window of time we slowly transition from the hard adjustment based on the residual at time T, we shift by the average residual between β_f and β_p over a window of time in the past. More specifically, define $r(t)$ as

$$r(t) = \log\left(\frac{\beta_f(t)}{\beta_p(t)}\right), \quad t \le T$$

and $\beta_{F_1}(t)$ and $\beta_{F_2}(t)$ as:

$$\beta_{F_1}(t) = \exp\big(r(T)\big)\,\beta_p(t), \quad t \ge T$$
$$\beta_{F_2}(t) = \exp\left(\frac{1}{n}\sum_{i=1}^{n} r(T-i+1)\right)\beta_p(t), \quad t \ge T$$

and transition weights $w(t)$ as

$$w(t) = \begin{cases} \dfrac{M-(t-T)}{M}, & T \le t \le T+M \\ 0, & otherwise \end{cases}$$

Then, for a given n and M, we define $\beta_F(t)$ as

$$\beta_F(t) = w(t)\beta_{F_1}(t) + \big(1-w(t)\big)\beta_{F_2}(t)$$

Based on out-of-sample tests similar to those described in the sensitivity analyses for optimal values of M and n, we found that the optimal n was 42 and the optimal M was for M to be, by draw, drawn from a uniform distribution of windows from 7 to 28 days.

SEIR-predict

The general format of our predictions is relatively simple: we take the final predicted β_F and run our system of ODEs forward in time using our fitted compartment values at time T as the initial conditions of the second SEIR model.

There are however a number of simplifications made within our modeling formulation. First, we ignore the potential for importation which may be more likely in larger, more dense locations. Second, we assume a well-mixed population which may be more egregious in smaller, less dense locations. As two intermediate solutions for this, we introduce two correction factors. In each location we only use one or the other correction factor, and the use and magnitude of the correction is based on OOS predictive validity dropping 8 weeks of data and comparing the predicted outbreak to the observed one. The first correction factor allows for the addition of a small number of additional infections above and beyond those from the interaction between I_1 and I_2 and S. These can be envisaged as individuals traveling outside the location, becoming infected, and returning as exposed individuals. The second correction factor removes a small fraction of exposed individuals from the E compartment and moves them directly to the recovered compartment. Our model acts on the fraction of individuals who are infectious, exposed, etc, and the results of allowing for fractional infectious individuals (and no possibility for truly 'zero' infections) can alter the dynamics for small locations. These corrections can be mathematically described using θ^+ and θ^- for the importation correction and the small location correction, respectively. Again, each location receives only one of these and they alter the SEIR model formulation for prediction as:

$$\frac{dS}{dt} = -\beta(t)\frac{S(I_1 + I_2)^\alpha}{N} - \theta^+ S$$
$$\frac{dE}{dt} = \beta(t)\frac{S(I_1 + I_2)^\alpha}{N} - \sigma E + \theta^+ S - \theta^- E$$
$$\frac{dI_1}{dt} = \sigma E - \gamma_1 I_1$$
$$\frac{dI_2}{dt} = \gamma_1 I_1 - \gamma_2 I_2$$
$$\frac{dR}{dt} = \gamma_2 I_2 + \theta^- E$$

With these correction factors identified, we can then run our ODEs forward (again using the Runge-Kutta 4 algorithm), to have a complete time-series of infections through the end of the year.

Final data combination and summarization

The transmission model produces 1,000 full time series (including projections) of infections and deaths. We summarize draws into means and 95% UIs for reporting. To control for extreme values, the top 2.5% and bottom 2.5% of draws are dropped and replaced through random resampling of the remaining 950 draws.

Scenarios

We estimate the trajectory of the epidemic by state under a "mandates easing" scenario that models what would happen in each state if the current pattern of lifting social distancing mandates continues and new mandates are not imposed.

As a more plausible scenario, we use observations from the first phase of the pandemic to predict the likely response of state and local governments during the second phase. This plausible reference scenario assumes that in each location the trend of easing SDM will continue at its current trajectory until the daily death rate reaches a threshold of 8 deaths per million. If the daily death rate in a location exceeds that threshold, we assume that SDM will be reintroduced for a six-week period. The

choice of threshold (of a rate of daily deaths of 8 per million) represents the 90th percentile of the distribution of daily death rate at which locations implemented their mandates during the first months of the COVID-19 pandemic. We selected the 90th percentile rather than the 50th percentile to capture an anticipated increased reluctance from governments to re-impose mandates because of the economic effects of the first set of mandates. In locations that do not exceed the threshold of a daily death rate of 8 per million, the projection is based on the covariates in model and the forecasts for these to December 31. In locations were the daily death rate exceeded 8 per million at the time of our final model run for this manuscript, we are assuming that mandates will be introduced within 7 days.

The scenario of universal mask wearing models what would happen if 95% of the population in each location always wore a mask when they were in public. This value was chosen to represent the highest observed rate of mask use observed globally during the COVID-19 pandemic through July 2020. In this scenario, we also assume that if the daily death rate in a state exceeds 8 deaths per million, SDMs will be reintroduced for a six-week period.

Alternate mask use scenario

The universal mask wearing scenario assumes 95% population coverage of mask use when outside the home. This level of mask use is based on the highest observed proportion during the study period, occurring in Singapore. However, most countries remain far from that level of mask use. We also explored a scenario of 85% population coverage. That level also corresponds to roughly the 85th percentile of the mask use coverage across all countries on July 21, the last day of mask use data in the model (86th percentile). SI Table 2 gives cumulative deaths in the two main scenarios and this third scenario for January 1, 2021 globally and by GBD super regions. SI Figure 8 shows the results of this alternative mask use scenario globally and by GBD super regions.

SI Table 3. Results from the two main scenarios presented in the main text and a third alternative scenario where mask use achieved 85% coverage within 7 days of the model projection. Results are presented as cumulative deaths on January 1, 2021.

Region	Reference (95% UI)	Universal mask use (95% UI)	Alternative mask use (95% UI)
Global	3226003 (2183429-5221802)	2085710 (1529000-3183895)	2359967 (1697510-3673747)
Southeast Asia, East Asia, and Oceania	125200 (46949-292524)	87591 (30757-238976)	102870 (38844-264347)
Central Europe, Eastern Europe, and Central Asia	232097 (131801-436407)	69468 (50952-92898)	90172 (64013-133718)
High-income	738007 (565234-1130053)	519447 (461394-634322)	536495 (473086-668933)
Latin America and Caribbean	516094 (434664-614954)	446680 (383343-518128)	488043 (419130-571336)
North Africa and Middle East	326138 (203558-552056)	137336 (88545-235416)	167892 (112826-286478)
South Asia	1108806 (519804-2256104)	751373 (345092-1638252)	875027 (403383-1847628)
Sub-Saharan Africa	179661 (75559-352596)	73816 (33761-157277)	99469 (42963-213231)

SI Figure 15. Cumulative deaths from January 1 2020 to January 1 2021 in the reference, universal mask use scenario (95% coverage), and an alternative 85% mask use coverage scenario.